

CONTACT ANGLE CHANGE and WETTING of DROPLETS on  
PLANAR SURFACES

by

Fatih Pelik

A Thesis Submitted to the  
Graduate School of Sciences  
in Partial Fulfillment of the Requirements for  
the Degree of

Master of Science

in

Physics

Koç University

September, 2010

Koç University  
Graduate School of Sciences and Engineering

This is to certify that I have examined this copy of a master's thesis by

Fatih Pelik

and have found that it is complete and satisfactory in all respects,  
and that any and all revisions required by the final  
examining committee have been made.

Committee Members:

---

Assoc. Prof. Özgür E. Müstecaplıođlu

---

Assoc. Prof. Alper Kiraz

---

Assoc. Prof. Metin Muradođlu

Date: \_\_\_\_\_

*To my friends*

## ABSTRACT

In this thesis, we have studied contact angle behavior of droplets on ideal and rough surfaces. We have examined contact angles on both homogeneous rough surfaces and heterogeneous rough surfaces. Then, we have studied how the contact angles of droplets change if we apply an external potential to the surface where the droplet rests. Splitting of a droplet has also been studied. To do that, first we have rederived some formulas and with the help of these formulas we have figured out how to split the droplets. Also, we have calculated the electrostatic forces and capacitive energies on an ewod-actuated droplet. Finally, we have calculated the forces acting on the liquid-droplet interface of a droplet which is immersed in a liquid. These calculations have been done for three different cases.

## ÖZETÇE

Bu çalışmada, damlacıkların kontakt açılarının kusursuz ve pürüzlü yüzeylerde nasıl davrandığını inceledik. Kontakt açılarının homojen ve heterojen yüzeylerde nasıl davrandığını inceledik. Daha sonra, damlacıkların üzerinde bulunduğu yüzeye bir potansiyel uygularsak açının nasıl değişeceğine baktık. Damlacığın nasıl bölünebileceği konusu da çalışıldı. Bunu yapabilmek için öncelikle bazı formülleri elde ettik ve bu formüller yardımıyla damlacığın nasıl bölüneceğini öğrendik. Ayrıca, ewod yöntemiyle harekete geçirilen damlacık üzerine etki eden kuvvetleri ve kapasitif enerjileri hesapladık. Son olarak da, başka bir sıvı içerisine daldırılmış bir damlacığın sıvı-damlacık yüzeyine etki eden kuvvetleri hesapladık. Bu hesaplamalar üç ayrı durum için yapıldı.

## ACKNOWLEDGMENTS

First of all, I would like to thank to my advisor Assoc. Prof. Özgür E. Müstecaplıođlu for his guidance and teaching. He has always been supportive and understanding towards me, and his encouragement helped me a lot in writing my thesis. I would also like to thank to my thesis committee for taking the time to review my thesis.

I would like to thank to Prof. Alphan Sennarođlu for his suggestions and comments in my thesis.

I would also like to give my special thanks to my physicist friends Ramazan Uzel, Mustafa Gündođan, Neslihan Oflaz, Őeyda İpek, Ozan Sarıyer, Ahad Khaleghi, Yasa EkŐiođlu, Enes Uysal, Saber Rostamzadeh, Omid Khosravani, NeŐe Aral, Seçil Gürkan, Duygu Can, UlaŐ Gökay, Ongun Özçelik, Yasin Karadađ and Utkan Güngördü. We always had nice moments together. I will never forget the time I spent with you.

I would also like to thank to my other friends who were always more than friends to me. We really enjoyed having nice talks, nice coffee breaks and of course unforgettable parties.

I would like to thank to our lab. coordinator Nazmi Yılmaz for his gentle attitude.

I would like to thank to TUBITAK (The Scientific and Technological Research Council of Turkey) for providing the graduate scholarship during my M.S. study.

Finally, I would like to thank to my parents, İlknur Pelik and Nazım Pelik and my sister Merve Pelik, for their endless support and love that made me reach my goals in my life.

## TABLE OF CONTENTS

<b>List of Figures</b>	<b>ix</b>
<b>Chapter 1: Introduction</b>	<b>1</b>
<b>Chapter 2: Contact Angle on Ideal and Rough Surfaces</b>	<b>3</b>
2.1 Contact Angle . . . . .	3
2.2 Wenzel's Model . . . . .	6
2.3 Cassie-Baxter Method . . . . .	7
<b>Chapter 3: Contribution of Energy and Entropy to the Electrical Double Layer</b>	<b>8</b>
3.1 Electrical Double Layer . . . . .	8
3.2 The Energy . . . . .	9
3.3 The Entropy . . . . .	10
3.4 Single Flat Double Layer . . . . .	11
<b>Chapter 4: Splitting a Liquid Droplet</b>	<b>14</b>
4.1 Electrowetting . . . . .	14
4.2 Splitting a Droplet . . . . .	16
4.3 Contact Angle Change . . . . .	19
4.4 Optimizing the Channel Gap . . . . .	21
<b>Chapter 5: Calculation of Electrostatic Forces and Capacitive Energies for an EWOD-Actuated Droplet</b>	<b>22</b>
<b>Chapter 6: Charge-Related Wetting Phenomena</b>	<b>29</b>
6.1 Constant Potential Case (Case I) . . . . .	30
6.2 Constant Charge Case (Case II) . . . . .	33

6.3 Electrowetting on Dielectrics (EWOD) Case (Case III) . . . . .	34
<b>Chapter 7: Conclusion</b>	<b>37</b>
<b>Bibliography</b>	<b>38</b>



## LIST OF FIGURES

1.1	Lotus Effect . . . . .	1
2.1	Contact angle . . . . .	3
2.2	Relation between contact angle and wettability . . . . .	4
2.3	Contact angle hysteresis . . . . .	5
2.4	a) Cassie state, b) Wenzel state, [6] . . . . .	6
2.5	Displacement of the contact line, [4] . . . . .	6
3.1	Electrical Double Layer, [5] . . . . .	8
4.1	a) No applied potential, b) Under applied potential . . . . .	14
4.2	Contact angle change according to the Lippmann equation . . . . .	16
4.3	Droplet in a microchannel [14]. (a) Top view, (b) Cross-sectional view, (c) After energizing electrodes . . . . .	17
4.4	Channel I System, [14] . . . . .	20
4.5	Channel II System, [14] . . . . .	20
4.6	Optimizing the channel gap to have a reliable splitting, [13] . . . . .	21
5.1	Conducting droplet in EWOD configuration, [16] . . . . .	23
5.2	Forces acting on the droplet when $C_l \ll C_u$ , $C_l = C_u$ , and $C_l \gg C_u$ . . . . .	25
5.3	Capacitive energies for the droplet when $C_l \ll C_u$ , $C_l = C_u$ , and $C_l \gg C_u$ . . . . .	27
6.1	Charge Related Wetting Phenomena . . . . .	29
6.2	Control Surfaces of the System, [17] . . . . .	30
6.3	Control Surfaces of EWOD System, [17] . . . . .	34

## Chapter 1

## INTRODUCTION

In the beginning of the 19th century, Laplace and Young proposed the existence of the term *interfacial energy* [23, 24, 25] and that term was the essence of wetting, which has become one of the hottest topics in the last 20 years [26, 27] because of some applications such as self-cleaning. Wetting is the result of intermolecular interactions when a liquid and a solid are brought together. If a liquid has a large surface tension or if it is put on a surface with low surface tension, it will have a small contact with the surface and form a spherical shape. However, droplets having low surface tension or droplets on a surface with high surface tension will maximize the contact with the surface.

Wetting has been studied for many years both theoretically [28, 29], and experimentally [30, 31]. Studying wetting properties of liquids on ideal surfaces is easier but in real life surfaces are not ideal but rough. Studying wetting properties and contact angle behavior of liquids is much harder on rough surfaces due to complications of roughness.



Figure 1.1: Lotus Effect

As we said before, self cleaning of the surfaces is a very important area to investigate. Some plant leaves such as, lotus plant leaves, raspberry leaves and strawberry leaves are

known as water repellents because they eliminate the water droplets. When a water droplet comes on the leaf, the droplet minimizes the contact with the leaf and starts rolling over the leaf and while rolling, it washes off the contamination very effectively as seen in Fig. (1.1). Water repellent surfaces are very important in many areas, such as prevention of adhesion of snow, self-cleaning windows, rain drops on planes.

For a droplet to start rolling, it should have a small contact angle hysteresis. The contact angle hysteresis and the apparent contact angle depend on the surface where the droplet rests. The surface roughness has a strong effect on the contact angle hysteresis of droplets and it has been studied by many researchers [32, 33] in order to develop superhydrophobic surfaces. If we can combine hydrophobicity and roughness cleverly, we can have droplets which can remain nearly spherical on substrates [34, 35, 36, 37].

Fluidic control at small scales is also very important due to its potential applications such as chemical analysis. In chemical analysis, it is preferred to use small droplets rather than continuous flows, because it is more efficient and easier to control. Electrowetting, EWOD, is the most promising actuation method where the droplet can be carried on flat surfaces or between two plates.

## Chapter 2

## CONTACT ANGLE ON IDEAL AND ROUGH SURFACES

In this section, we briefly explain what a contact angle is and how it behaves on ideal and rough surfaces. We also discuss hydrophobic and hydrophilic surfaces and which features of droplets tell us whether the surface is more hydrophobic or not. Contact angles of the same droplet on homogeneous and heterogeneous surfaces act differently and we derived contact angle formulas of droplets on these surfaces.

**2.1 Contact Angle**

Adhesive forces are considered between two bodies. If we consider glass and water, attractive forces between them cause the water to spread across the surface. But cohesive forces are internal forces of a body, which results due to the attraction of the molecules of it. Cohesive forces cause the water drop to have a spherical shape and avoid contact with the surface. So, we can say that the contact angle of a droplet on a substrate is the result of adhesive and cohesive forces. The contact angle  $\theta$ , as seen in Fig. (2.1), is the angle between liquid-vapor interface and solid-liquid interface. In Fig. (2.2) we can see that when the drop spreads over the surface contact angle decreases. So, we can say that contact angle has an inverse measure of wettability.

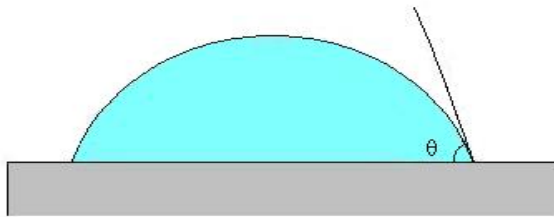


Figure 2.1: Contact angle

For low contact angles ( $\theta < 90^\circ$ ), the wetting is propitious and the droplet spreads on a large portion of the substrate. For high contact angles ( $\theta > 90^\circ$ ) the wetting is poor, so the droplet will not spread over the substrate and minimize the contact. For water droplets if the surface is wettable we can call the surface as "hydrophilic" but if the surface is non-wettable we can call it as "hydrophobic". There is also one more surface called as "superhydrophobic" on which the contact angle of a water droplet is higher than  $150^\circ$ . Water droplets on superhydrophobic surfaces have almost no contact with the surface.

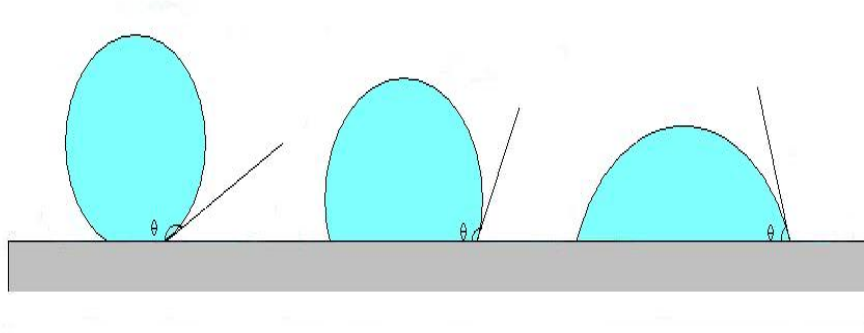


Figure 2.2: Relation between contact angle and wettability

We can separate the solids into two groups: the first one is high energy solids. Solids such as metals are hard solids because bonds within the solids are very strong. Most liquids show low contact angle, thus high wettability on high energy solids. The second group is low energy solids. The bonds within these solids are weak. Liquids on low energy solids can either have complete or partial wetting.

In 1805, Young and Laplace proposed existence of the "surface energy" term which is the excess energy of a material at the surface [1]. If gravity effect is neglected, a droplet on an ideal substrate will form a spherical cap. By ideal, we mean that the substrate is flat, rigid, perfectly smooth and chemically homogeneous. Contact angle,  $\theta$ , of a droplet on an ideal surface was proposed by Thomas Young two hundred years ago [2];

$$\cos \theta = \frac{\gamma_{SV} - \gamma_{SL}}{\gamma_{LV}} \quad (2.1)$$

where  $\gamma_{SV}$ ,  $\gamma_{SL}$ , and  $\gamma_{LV}$  are solid-vapor, solid-liquid, and liquid-vapor interfacial tensions respectively.

Unlike described above, solids are not ideal but rough, which affects their wettability very much [3]. The wettability is affected by not only non-ideality of surfaces but also droplets containing different chemical species such as surfactants [4]. Droplets remaining stuck on a tilted surface can be given as an example for the result of non-ideality of the surface. For this situation the droplet has two contact angles; advancing contact angle  $\theta_a$ , and receding contact angle  $\theta_r$ . We can observe advancing and receding contact angles in the following way; first we put the droplet on a substrate and start tilting the substrate. When the droplet starts moving, the angle in the leading face of the droplet is the advancing contact angle and the angle in the rear part of the droplet is the receding contact angle as in Fig. (2.3). Shortly, maximum and minimum contact angle values are called advancing and receding contact angles respectively. The difference of advancing contact angle and receding contact angle is called as "contact angle hysteresis" which is shown by  $H$ . ( $H = \theta_a - \theta_r$ ). Contact angle hysteresis is a very important parameter [4] and we can explain this importance with an example. Let us assume we have two different surfaces. When we put a droplet on the first surface let the contact angle be  $\theta_1 = 170^\circ$ , and let the contact angle of the same droplet be  $\theta_2 = 150^\circ$  on the second surface. First surface seems more hydrophobic than the second surface due to the larger contact angle. However, the second surface might be more hydrophobic. To understand this let us start tilting the surfaces. If the contact angle hysteresis of the first droplet,  $H_1$ , is large the droplet remains stuck on the tilted surface. However, if the contact angle hysteresis of the second droplet,  $H_2$ , is very low the droplet starts rolling on the surface. Because  $H_1 > H_2$ , we conclude that the second surface is more hydrophobic. So, to discuss whether a surface is superhydrophobic or not we should not only mention its contact angle but also its contact angle hysteresis [5].

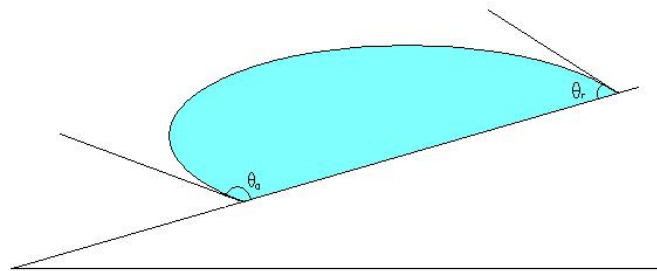


Figure 2.3: Contact angle hysteresis

Rough surfaces can be split into two categories: homogeneous and heterogeneous surfaces. On homogeneous rough surfaces, the liquid fills the roughness of the surface. However, on the heterogeneous rough surfaces there is air in the roughness, so the liquid is in contact with both air and the surface. Wenzel and Cassie-Baxter methods try to explain how the contact angles of droplets behave on homogeneous and heterogeneous surfaces respectively. [1, 3, 4, 6]

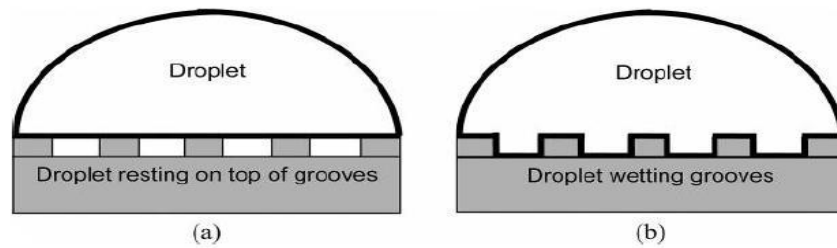


Figure 2.4: a) Cassie state, b) Wenzel state, [6]

## 2.2 Wenzel's Model

Wenzel proposed a model to understand how the roughness affects contact angle of a droplet. He assumed a substrate with roughness  $r$ , which is defined as the surface area of the solid over its apparent surface area. The contact angle,  $\theta^*$ , of the droplet on this rough surface can be calculated by assuming a small displacement  $dx$  of the contact line as in Fig. (2.5). The displacement will cause a change in the surface energy [4]:

$$dE = r(\gamma_{SL} - \gamma_{SV})dx + \gamma_{LV}dx \cos \theta^* \quad (2.2)$$

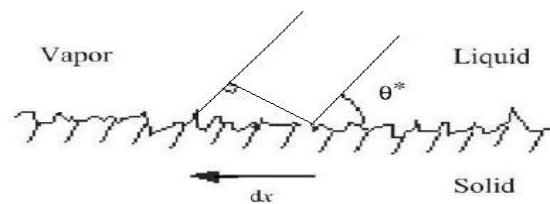


Figure 2.5: Displacement of the contact line, [4]

We know that, E will be minimum at equilibrium. By substituting Young's law  $\gamma_{SV} - \gamma_{SL} = \gamma_{LV} \cos \theta$  in the equation above we get the Wenzel's relation;

$$\begin{aligned} 0 &= -\gamma_{LV} r \cos \theta dx + \gamma_{LV} dx \cos \theta^* \\ \cos \theta^* &= r \cos \theta \end{aligned} \quad (2.3)$$

This relation tells us that if a droplet is put on an ideal hydrophilic surface ( $\theta < 90^\circ$ ), the following relation holds true;  $\theta^* < \theta < 90^\circ$ . If the same droplet is put on an ideal hydrophobic surface ( $\theta > 90^\circ$ ), the relation is  $\theta^* > \theta > 90^\circ$

### 2.3 Cassie-Baxter Method

In this model the air is trapped in cavities and the liquid is in contact with both air and solid. In this case [1],

$$\begin{aligned} \gamma_{SV} &\rightarrow r\gamma_{SV} \\ \gamma_{SL} &\rightarrow \phi r\gamma_{SL} + (1 - \phi)(r\gamma_{SV} + \gamma_{LV}) \end{aligned}$$

where  $\phi$  is the fraction of the area where the liquid is in contact with the solid. If we substitute these relations in Eq. (2.1) we get;

$$\begin{aligned} \cos \theta^* &= \frac{r\gamma_{SV} - \phi r\gamma_{SL} - (1 - \phi)(r\gamma_{SV} + \gamma_{LV})}{\gamma_{LV}} \\ &= \frac{r\gamma_{SV} - \phi r\gamma_{SL} - r\gamma_{SV} - \gamma_{LV} + \phi r\gamma_{SV} + \phi\gamma_{LV}}{\gamma_{LV}} \\ &= \frac{\phi r(\gamma_{SV} - \gamma_{SL}) + \gamma_{LV}(\phi - 1)}{\gamma_{LV}} \\ &= \frac{\phi r\gamma_{LV} \cos \theta + \gamma_{LV}(\phi - 1)}{\gamma_{LV}} \\ \cos \theta^* &= \phi(r \cos \theta + 1) - 1 \end{aligned} \quad (2.4)$$

Note that when  $\phi = 1$ , Eq. (2.4) reduces to Eq. (2.3). We have seen that roughness can make a hydrophobic surface more hydrophobic. For example, if the contact angle of a droplet on an ideal surface is around  $120^\circ$ , it can be as high as  $150^\circ$  on a rough surface. Both of the methods above explains this effect.



## Chapter 3

## CONTRIBUTION OF ENERGY AND ENTROPY TO THE ELECTRICAL DOUBLE LAYER

### 3.1 *Electrical Double Layer*

When we bring a liquid, which contains free ions, and a solid in contact, due to van der Waals forces, adsorption of ions and water molecules occurs. As a result, a layer which consists of a region with a net surface charge bound to solid and another region above it is formed. This layer is called *electrical double layer* [5]. If we have a solid surface which is electrically charged, because of the attraction of the ions, having opposite charge, to the surface and repulsion of the ions, having the same charge, away from the surface, electrical double layer is formed. The lower layer is called *Stern layer* and the other layer is called *diffuse layer*. Adsorption of water molecules does not introduce a net surface charge. If we have a solution which contains ion types,  $i$ , with charge number,  $z_i$ , in mole fraction,  $x_i$  the thickness of the diffuse layer, as seen in Fig. (3.1), is called Debye length,  $1/K$ , where

$$K^2 = \frac{\sum_i n_{i0} z_i^2 e^2}{\epsilon_r \epsilon_0 kT}$$

where  $n$  is the concentration of ions,  $\epsilon_0$  the vacuum permittivity,  $\epsilon_r$  the dielectric constant of the solution.

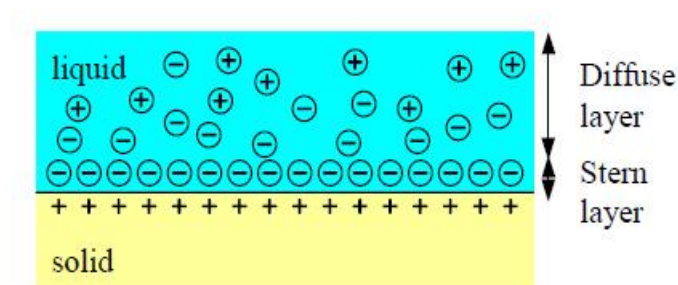


Figure 3.1: Electrical Double Layer, [5]

### 3.2 The Energy

In order to calculate the energy contribution to the double layer let us define dimensionless potentials as  $\psi = \frac{e\varphi}{kT}$ , and  $\psi_0 = \frac{e\varphi_0}{kT}$ . Also, surface charge density relation states that [9],

$$\sigma = -\epsilon_r \epsilon_0 \nabla_n \varphi = -\epsilon_r \epsilon_0 \frac{d\varphi}{dn} \quad (3.1)$$

where  $n$  is the normal of the surface.

The Green's theorem tells us that [7],

$$-\int_A (a_0 \nabla_n b) dA = \int_V (a \nabla^2 b + \nabla a \cdot \nabla b) dV \quad (3.2)$$

where  $a$  and  $b$  are scalar fields. These fields vanish at infinity and have values  $a_0$ , and  $b_0$  at the surface. We also need Poisson's equation for some future calculations,

$$\nabla^2 \varphi = -\frac{\rho}{\epsilon_r \epsilon_0} \quad (3.3)$$

The electrostatic energy,  $U_{el}$ , can be written as [8],

$$U_{el} = \frac{\epsilon_r \epsilon_0}{2} \int_V (\nabla \varphi)^2 dV$$

By using Green's theorem we get,

$$U_{el} = -\frac{\epsilon_r \epsilon_0}{2} \int_A \varphi_0 \left( \frac{\partial \varphi}{\partial n} \right)_{surf} dA - \frac{\epsilon_r \epsilon_0}{2} \int_V \varphi (\nabla^2 \varphi) dV$$

If we substitute Eq. (3.1), and Eq. (3.3) in the equation above,

$$U_{el} = -\frac{\epsilon_r \epsilon_0}{2} \int_A \varphi_0 \left( \frac{-\epsilon_r \epsilon_0}{-\epsilon_r \epsilon_0} \right) \left( \frac{\partial \varphi}{\partial n} \right) dA - \frac{\epsilon_r \epsilon_0}{2} \int_V \varphi \left( \frac{-\rho}{\epsilon_r \epsilon_0} \right) dV$$

Finally,

$$U_{el} = \frac{1}{2} \int_A \varphi_0 \sigma dA + \frac{1}{2} \int_V \varphi \rho dV \quad (3.4)$$

We can get Poisson-Boltzmann equation, Eq. (3.5), by using the equation below,

$$\nabla^2 \varphi = -\frac{\rho}{\epsilon_r \epsilon_0} = -\frac{\sum_i z_i e n_i}{\epsilon_r \epsilon_0} = -\frac{\sum_i z_i e n_{i0} \exp(-z_i e \varphi / kT)}{\epsilon_r \epsilon_0}$$

For a single z-z electrolyte we can rewrite the equation as,

$$\begin{aligned} \nabla^2 \varphi &= -\frac{z e n_0}{\epsilon_r \epsilon_0} \exp(-z e \varphi / kT) + \frac{z e n_0}{\epsilon_r \epsilon_0} \exp(z e \varphi / kT) \\ &= \frac{z e n_0}{\epsilon_r \epsilon_0} [\exp(z e \varphi / kT) - \exp(-z e \varphi / kT)] \end{aligned}$$

$$\begin{aligned}
&= 2 \frac{ze n_0}{\epsilon_r \epsilon_0} \sinh(ze\varphi/kT) \\
&= 2 \frac{ze n_0}{\epsilon_r \epsilon_0} \left(\frac{ze}{ze}\right) \left(\frac{kT}{kT}\right) \sinh(ze\varphi/kT) \\
&= 2 \frac{z^2 e^2 n_0}{\epsilon_r \epsilon_0 kT} \left(\frac{kT}{ze}\right) \sinh(z\psi) \\
\nabla^2 \varphi &= K^2 \frac{kT}{ze} \sinh(z\psi) \tag{3.5}
\end{aligned}$$

### 3.3 The Entropy

The entropy difference,  $\Delta S$ , between the ion distribution in the double layer and solvent molecules at  $\varphi = 0$  can be written for dilute solutions by [8],

$$\begin{aligned}
\Delta S &= -k \int_V \left[ \sum_i n_i \ln \left( \frac{x_i}{x_{i0}} \right) + n_w \ln \left( \frac{1 - \sum_i x_i}{1 - \sum_i x_{i0}} \right) \right] dV \\
&\cong -k \int_V \left[ \sum_i \left( n_i \ln \left( \frac{n_i}{n_{i0}} \right) - n_i + n_{i0} \right) \right] dV
\end{aligned}$$

By using the relations,  $n_i = n_{i0} e^{-z_i e\varphi/kT}$ , and  $\psi = \frac{e\varphi}{kT}$

$$\begin{aligned}
\Delta S &= -k \int_V \left[ \sum_i \left( n_{i0} e^{-z_i \psi} \ln \left( \frac{n_{i0} e^{-z_i \psi}}{n_{i0}} \right) - n_{i0} e^{-z_i \psi} + n_{i0} \right) \right] dV \\
&= -k \int_V \left[ \sum_i \left( n_{i0} e^{-z_i \psi} (-z_i \psi) - n_{i0} e^{-z_i \psi} + n_{i0} \right) \right] dV \\
&= k \int_V \left[ \sum_i n_{i0} (z_i \psi e^{-z_i \psi} + e^{-z_i \psi} - 1) \right] dV \tag{3.6}
\end{aligned}$$

We know that,

$$\rho = \sum_i z_i e n_i = -\epsilon_r \epsilon_0 \nabla^2 \varphi \tag{3.7}$$

If we integrate the equation above over  $(0, \psi)$  we get,

$$\int_0^\psi \epsilon_r \epsilon_0 \nabla^2 \varphi d\psi = - \int_0^\psi \rho d\psi = \int_0^\psi \sum_i e n_{i0} e^{-z_i \psi} d(-z_i \psi) = \sum_i e n_{i0} (e^{-z_i \psi} - 1) \tag{3.8}$$

Let us multiply Eq. (3.6) by  $-T$  and separate the integral into two parts,

$$\begin{aligned}
-T\Delta S &= -kT \int_V \left[ \sum_i n_{i0} (z_i \psi e^{-z_i \psi} + e^{-z_i \psi} - 1) \right] dV \\
&= -kT \int_V \sum_i n_{i0} z_i \psi e^{-z_i \psi} dV - kT \int_V \left[ \sum_i n_{i0} (e^{-z_i \psi} - 1) \right] dV
\end{aligned}$$

By using Eq. (3.7) and Eq.(3.8)

$$\begin{aligned}
&= -kT \int_V \sum_i n_{i0} z_i \left(\frac{e}{e}\right) \psi e^{-z_i \psi} dV - kT \left(\frac{e}{e}\right) \int_V \left[ \sum_i n_{i0} e^{-z_i \psi} - 1 \right] dV \\
&= -kT \int_V \left(\frac{\psi}{e}\right) (-\epsilon_r \epsilon_0) \nabla^2 \varphi dV - \frac{kT}{e} \int_V dV \int_0^\psi \epsilon_r \epsilon_0 \nabla^2 \varphi d\psi \\
\psi &= \frac{e\varphi}{kT} \Rightarrow d\psi = \frac{e}{kT} d\varphi
\end{aligned}$$

$$-T\Delta S = kT \int_V \frac{e\varphi}{kT} \frac{1}{e} \epsilon_r \epsilon_0 \nabla^2 \varphi dV - \frac{kT}{e} \int_V dV \int_0^\psi \epsilon_r \epsilon_0 \nabla^2 \varphi \frac{e}{kT} d\varphi$$

Finally we get,

$$-T\Delta S = \epsilon_r \epsilon_0 \int_V \varphi \nabla^2 \varphi dV - \epsilon_r \epsilon_0 \int_V dV \int_0^\varphi \nabla^2 \varphi d\varphi \quad (3.9)$$

### 3.4 Single Flat Double Layer

We can write the electrostatic free energy of a single flat double layer in a 1-1 electrolyte of concentration  $n$  as,

$$U_{el} = \frac{\epsilon_r \epsilon_0}{2} \int_{x=0}^{x=\infty} \left(\frac{d\varphi}{dx}\right)^2 dx = \frac{\epsilon_r \epsilon_0}{2} \int_{\varphi=\varphi_0}^{\varphi=0} \left(\frac{d\varphi}{dx}\right) d\varphi \quad (3.10)$$

For this case, the solution of the Poisson-Boltzmann equation giving the first integral is,

$$\frac{d\varphi}{dx} = -2K \frac{kT}{e} \sinh\left(\frac{e\varphi}{2kT}\right) \quad (3.11)$$

If we substitute Eq. (3.11) in Eq. (3.10), we get

$$\begin{aligned}
U_{el} &= \frac{\epsilon_r \epsilon_0}{2} \int_{\varphi=\varphi_0}^{\varphi=0} -2K \frac{kT}{e} \sinh\left(\frac{e\varphi}{2kT}\right) d\varphi \\
&= -\epsilon_r \epsilon_0 K \frac{kT}{e} \frac{2kT}{e} \cosh\left(\frac{e\varphi}{2kT}\right) \Big|_{\varphi=\varphi_0}^{\varphi=0} \\
&= -2\epsilon_r \epsilon_0 K \left(\frac{kT}{e}\right)^2 \left(1 - \cosh\left(\frac{e\varphi_0}{2kT}\right)\right) \\
U_{el} &= 2\epsilon_r \epsilon_0 K \left(\frac{kT}{e}\right)^2 \left(\cosh\left(\frac{e\varphi_0}{2kT}\right) - 1\right) \quad (3.12)
\end{aligned}$$

Let us multiply Eq. (3.6) by  $-T$  and do the summation for this case,

$$\begin{aligned}
-T\Delta S &= -kT \int_{x=0}^{\infty} n(\psi e^{-\psi} + e^{-\psi} - 1 - \psi e^{\psi} + e^{\psi} - 1) dx \\
&= -nkT \int_{x=0}^{\infty} [\psi(e^{-\psi} - e^{\psi} + (e^{\psi} + e^{-\psi}) - 2)] dx
\end{aligned}$$

$$\begin{aligned}
&= -nkT \int_{x=0}^{\infty} [-2\psi \sinh(\psi) + 2 \cosh(\psi) - 2] dx \\
&= 2nkT \int_{x=0}^{\infty} [\psi \sinh(\psi) - \cosh(\psi) + 1] dx \tag{3.13}
\end{aligned}$$

By using the relations,  $\frac{d\varphi}{dx} = -2K \frac{kT}{e} \sinh\left(\frac{e\varphi}{2kT}\right)$ , and  $\psi = \frac{e\varphi}{kT}$  we get,

$$\begin{aligned}
\frac{d}{dx} \left( \frac{e\varphi}{2kT} \right) &= -K \sinh\left(\frac{\psi}{2}\right) \\
\frac{d}{dx} \left( \frac{\psi}{2} \right) &= -K \sinh\left(\frac{\psi}{2}\right) \\
dx &= \frac{d\left(\frac{\psi}{2}\right)}{-K \sinh\left(\frac{\psi}{2}\right)}
\end{aligned}$$

If we substitute the relation above in Eq. (3.12) we get,

$$-T\Delta S = -\frac{2nkT}{K} \int_{\psi=\psi_0}^{\psi=0} \frac{(\psi \sinh(\psi) - \cosh(\psi) + 1)}{\sinh\left(\frac{\psi}{2}\right)} d\left(\frac{\psi}{2}\right)$$

By using the relation  $\cosh^2(x) - \sinh^2(x) = 1$

$$= -\frac{2nkT}{K} \int_{\psi=\psi_0}^{\psi=0} \frac{\left( \psi \sinh\left(\frac{\psi}{2} + \frac{\psi}{2}\right) - \cosh\left(\frac{\psi}{2} + \frac{\psi}{2}\right) + \cosh^2\left(\frac{\psi}{2}\right) - \sinh^2\left(\frac{\psi}{2}\right) \right)}{\sinh\left(\frac{\psi}{2}\right)} d\left(\frac{\psi}{2}\right)$$

We also know that,

$$\cosh(a + b) = \cosh(a) \cosh(b) + \sinh(a) \sinh(b)$$

$$\sinh(a + b) = \sinh(a) \cosh(b) + \sinh(b) \cosh(a)$$

$$\begin{aligned}
&= -\frac{2nkT}{K} \int_{\psi=\psi_0}^{\psi=0} \frac{\left( 2\psi \sinh\left(\frac{\psi}{2}\right) \cosh\left(\frac{\psi}{2}\right) - \cosh^2\left(\frac{\psi}{2}\right) - \sinh^2\left(\frac{\psi}{2}\right) \right)}{\sinh\left(\frac{\psi}{2}\right)} d\left(\frac{\psi}{2}\right) \\
&\quad - \frac{2nkT}{K} \int_{\psi=\psi_0}^{\psi=0} \frac{\left( \cosh^2\left(\frac{\psi}{2}\right) - \sinh^2\left(\frac{\psi}{2}\right) \right)}{\sinh\left(\frac{\psi}{2}\right)} d\left(\frac{\psi}{2}\right)
\end{aligned}$$

$$\begin{aligned}
&= -\frac{2nkT}{K} \int_{\psi=\psi_0}^{\psi=0} \left( 2\psi \cosh\left(\frac{\psi}{2}\right) - 2\sinh\left(\frac{\psi}{2}\right) \right) d\left(\frac{\psi}{2}\right) \\
&= 2nkKT \frac{\epsilon_r \epsilon_0 kT}{2ne^2} \int_{\psi=\psi_0}^{\psi=0} \left( 2\sinh\left(\frac{\psi}{2}\right) - 2\psi \cosh\left(\frac{\psi}{2}\right) \right) d\left(\frac{\psi}{2}\right) \\
&= 2\epsilon_r \epsilon_0 K \left(\frac{kT}{e}\right)^2 \int_{\psi=\psi_0}^{\psi=0} \left( \sinh\left(\frac{\psi}{2}\right) - \psi \cosh\left(\frac{\psi}{2}\right) \right) d\left(\frac{\psi}{2}\right)
\end{aligned}$$

If we change the variables,  $x = \frac{\psi}{2} \Rightarrow dx = \frac{d\psi}{2} \Rightarrow d\psi = 2dx$

$$= 2\epsilon_r \epsilon_0 K \left(\frac{kT}{e}\right)^2 \left[ \int_{x=\psi_0/2}^{x=0} \sinh(x) - \int_{x=\psi_0/2}^{x=0} 2x \cosh(x) \right] dx$$

By doing integration by parts  $x = u \Rightarrow dx = du$ ,  $\cosh(x)dx = dv \Rightarrow \sinh(x) = v$

$$\begin{aligned}
&= 2\epsilon_r \epsilon_0 K \left(\frac{kT}{e}\right)^2 \left[ \cosh(x) \Big|_{x=\psi_0/2}^{x=0} - 2 \left( x \sinh(x) \Big|_{x=\psi_0/2}^{x=0} - \int_{x=\psi_0/2}^{x=0} \sinh(x) dx \right) \right] \\
&= 2\epsilon_r \epsilon_0 K \left(\frac{kT}{e}\right)^2 \left[ 1 - \cosh\left(\frac{\psi_0}{2}\right) - 2 \left( \frac{\psi}{2} \sinh\left(\frac{\psi}{2}\right) \Big|_{\psi_0}^0 - \cosh\left(\frac{\psi}{2}\right) \Big|_{\psi_0}^0 \right) \right] \\
&= 2\epsilon_r \epsilon_0 K \left(\frac{kT}{e}\right)^2 \left[ 1 - \cosh\left(\frac{\psi_0}{2}\right) - 2 \left( 0 - \frac{\psi_0}{2} \sinh\left(\frac{\psi_0}{2}\right) - 1 + \cosh\left(\frac{\psi_0}{2}\right) \right) \right] \\
&= 2\epsilon_r \epsilon_0 K \left(\frac{kT}{e}\right)^2 \left[ 1 - \cosh\left(\frac{\psi_0}{2}\right) + \psi_0 \sinh\left(\frac{\psi_0}{2}\right) + 2 - 2 \cosh\left(\frac{\psi_0}{2}\right) \right] \\
-T\Delta S &= 2\epsilon_r \epsilon_0 K \left(\frac{kT}{e}\right)^2 \left[ 3 - 3 \cosh\left(\frac{\psi_0}{2}\right) + \psi_0 \sinh\left(\frac{\psi_0}{2}\right) \right] \tag{3.14}
\end{aligned}$$

Finally, we can calculate Helmholtz free energy,  $F_{el}$ , by adding Eq. (3.11) to Eq. (3.13)

$$\begin{aligned}
F_{el} &= U_{el} - T\Delta S \\
F_{el} &= 2\epsilon_r \epsilon_0 K \left(\frac{kT}{e}\right)^2 \left[ \cosh\left(\frac{\psi_0}{2}\right) - 1 + 3 - 3 \cosh\left(\frac{\psi_0}{2}\right) + \psi_0 \sinh\left(\frac{\psi_0}{2}\right) \right] \\
F_{el} &= 2\epsilon_r \epsilon_0 K \left(\frac{kT}{e}\right)^2 \left[ 2 - 2 \cosh\left(\frac{\psi_0}{2}\right) + \psi_0 \sinh\left(\frac{\psi_0}{2}\right) \right] \tag{3.15}
\end{aligned}$$

Let us assume we have a water droplet on a substrate. We can control the contact angle of this droplet by applying an electrical potential to the substrate. When we apply electrical potential, the force acting on the liquid-air interface can be calculated. This will be discussed in one of the subsequent chapters. Free energy (per unit surface area) equation, Eq. (3.15), also corresponds to the horizontal component of the force acting on the liquid-air interface.

## Chapter 4

## SPLITTING A LIQUID DROPLET

In order to split a droplet reliably, we have to know the theory of splitting very well. In this chapter, we rederived some mathematical formulas which help us to split a droplet in a microchannel. We also discussed which parameters help splitting process and the conditions in which the droplet can not be split.

**4.1 Electrowetting**

When we apply an electrical potential between a droplet and a surface, we observe that contact angle of the droplet changes as seen in Fig. (4.1). This phenomenon is called *electrowetting*. Electrowetting is treated as the charge-induced change in the interfacial energy between solid and liquid [5]. Lippmann recognised that capillary forces can be modified by adding electrostatic charges at an interface [10]. This situation is very important when it is applied to the case called electrowetting on dielectrics (EWOD). In this case the electrode is covered with an insulating film of microscopic thickness. When the electric voltage is applied, the electric charge is accumulated on the insulating layer causing a change in wettability and contact angle of the droplet.

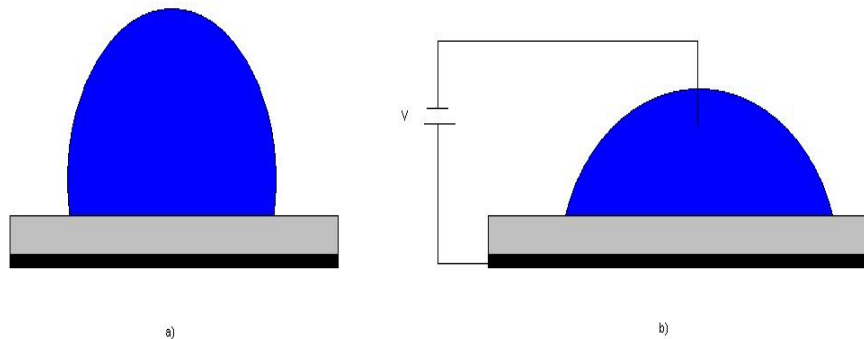


Figure 4.1: a) No applied potential, b) Under applied potential

According to Lippmann [10], the solid-liquid interfacial tension depends on the externally applied potential  $V$  as;

$$\gamma_{SL}(V) = \gamma_{SL}|_{V=0} - \frac{1}{2}CV^2 \quad (4.1)$$

where  $C$  is the capacitance of the dielectric layer. According to Young's equation, the relation between contact angle of the droplet and interfacial tensions:

$$\cos \theta = \frac{\gamma_{SV} - \gamma_{SL}}{\gamma_{LV}} \quad (4.2)$$

where  $\gamma_{SL}$ ,  $\gamma_{SV}$ , and  $\gamma_{LV}$  are solid-liquid, solid-vapor, and liquid-vapor interfacial tensions respectively.

If an external potential is applied to the system, Young's equation can be rewritten as:

$$\begin{aligned} \cos \theta^* &= \frac{\gamma_{SV} - \gamma_{SL}(V)}{\gamma_{LV}} \\ &= \frac{\gamma_{SV}}{\gamma_{LV}} - \frac{\gamma_{SL}(V)}{\gamma_{LV}} \\ &= \frac{\gamma_{SV}}{\gamma_{LV}} - \frac{\gamma_{SL}}{\gamma_{LV}} + \frac{CV^2}{2\gamma_{LV}} \\ \cos \theta^* &= \cos \theta + \frac{CV^2}{2\gamma_{LV}} \end{aligned}$$

where  $\theta$  is the contact angle when there is no external applied potential and  $C = \frac{\epsilon_0 \epsilon}{t}$ . Finally, the modified contact angle equation can be written as:

$$\cos \theta^* = \cos \theta + \frac{\epsilon_0 \epsilon}{2\gamma_{LV} t} V^2 \quad (4.3)$$

where  $\epsilon_0$  ( $8.85 \times 10^{-12} F/m$ ) is the permittivity of vacuum, and  $\epsilon$  the dielectric constant and  $t$  the thickness of the dielectric layer. From the equation above, we can see that contact angle decreases parabolically as the potential increases. But the contact angle is saturated at about  $80^\circ$ . Although there are some theories about why contact angle saturates [11, 12], the reason for the saturation is not clearly understood yet.



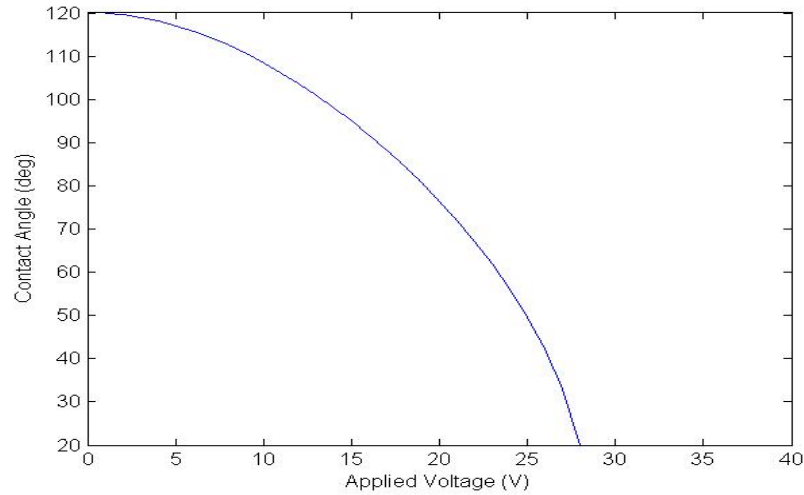


Figure 4.2: Contact angle change according to the Lippmann equation

## 4.2 Splitting a Droplet

To split a droplet, we need to put the droplet in a channel which consists of a top wall and a bottom wall. On the bottom wall, there should be electrodes covered with a hydrophobic dielectric layer. These electrodes are called “control electrodes”, because they control the splitting process. On the top wall, there should be a grounded electrode which is also covered with a hydrophobic dielectric layer. In order to split the droplet, it should be put in the channel and squeezed. The droplet must be in contact with both top and bottom wall at all times in order to complete the circuit. The solid-liquid interfacial area must occupy three electrodes as in Fig. (4.3 (c)). When the potential is applied on the left and right electrodes, while the middle electrode is left grounded, contact angles at three phase points decrease according to Eq. (4.3). If the contact angles at both sides decrease, they cause an increase of the radius of the curvature. Because the middle electrode is grounded during the process, it causes no contact angle change. The droplet wants to keep its total volume constant but the radius is getting larger, so it starts to shrink in the middle. We can say the splitting process starts with elongation of the droplet in the horizontal direction and necking of the droplet in the middle.

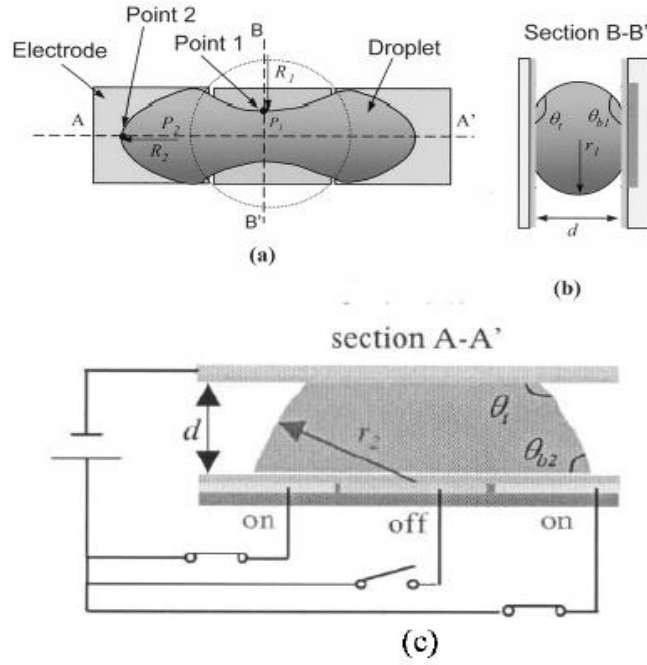


Figure 4.3: Droplet in a microchannel [14]. (a) Top view, (b) Cross-sectional view, (c) After energizing electrodes

The most important parameters to split a droplet are the distance between channels, the droplet size and contact angle change. We first need to understand the relation between these parameters in order to split the droplet reliably. For example, small channel gap helps the necking of the droplet. Also applying higher voltage results higher change in the contact angle and consequently helps the splitting process as well. If we use a large channel gap compared to droplet size we can not split the droplet.

The channel gap is geometrically related with the contact angles and radius of the meniscus curvature [13]:

$$r_1 = -\frac{d}{\cos \theta_t + \cos \theta_{b1}} \quad (4.4)$$

$$r_2 = -\frac{d}{\cos \theta_t + \cos \theta_{b2}} \quad (4.5)$$

where subscript 1 indicates the parameters in the middle region of the droplet and subscript 2 indicates the parameters in the right or left end region of the droplet. Here,  $\theta_t$  is the

contact angle on the top wall,  $\theta_b$  is the contact angle on the bottom wall and  $r$  is the principal radius of the curvature. We can now write the pressures in the middle and in the end regions related to the atmosphere pressure, principal radii and interfacial tension [14]:

$$P_1 - P_a = \gamma_{LV} \left( \frac{1}{r_1} + \frac{1}{R_1} \right) \quad (4.6)$$

$$P_2 - P_a = \gamma_{LV} \left( \frac{1}{r_2} + \frac{1}{R_2} \right) \quad (4.7)$$

where  $R$  is the principal radius of curvature as shown in Fig. (4.2 (a)), and  $P_a$  atmosphere pressure. In static equilibrium, pressures must be equal inside the droplet. Now if we subtract Eq. (4.7) from Eq. (4.6):

$$\begin{aligned} P_1 - P_2 = 0 &= \gamma_{LV} \left( \frac{1}{r_1} + \frac{1}{R_1} \right) - \gamma_{LV} \left( \frac{1}{r_2} + \frac{1}{R_2} \right) \\ &\Rightarrow \gamma_{LV} \left[ \left( \frac{1}{r_1} - \frac{1}{r_2} \right) + \left( \frac{1}{R_1} - \frac{1}{R_2} \right) \right] = 0 \end{aligned}$$

From the equations (4.4) and (4.5) we can write,

$$\frac{1}{r_1} - \frac{1}{r_2} = \frac{\cos \theta_{b2} - \cos \theta_{b1}}{d}$$

If we put this relation in the equation above, we get:

$$0 = \gamma_{LV} \left( \frac{1}{R_1} - \frac{1}{R_2} + \frac{\cos \theta_{b2} - \cos \theta_{b1}}{d} \right) \quad (4.8)$$

Finally, we can write the channel gap related to the difference of contact angles and radii of curvature:

$$\frac{1}{R_1} = \frac{1}{R_2} - \frac{\cos \theta_{b2} - \cos \theta_{b1}}{d} \quad (4.9)$$

On the right side of the droplet or on the left side of the droplet the contact angle change under the applied potential can be written as:

$$\cos \theta_{b2}(V) = \cos \theta_{b2}|_{V=0} + \frac{\epsilon_0 \epsilon V^2}{2\gamma_{LV} t} \quad (4.10)$$

We don't energize the middle droplet, so the contact angle of the middle part of the droplet does not change and it is equal to the contact angle of the right or left side of the droplet when there is no applied potential:

$$\theta_{b1} = \theta_{b2}|_{V=0}$$

So, we can write,

$$\cos \theta_{b2} - \cos \theta_{b1} = \cos \theta_{b2} - \cos \theta_{b2}|_{V=0} = \frac{\epsilon_0 \epsilon V^2}{2\gamma_{LV}t} \quad (4.11)$$

If we substitute Eq. (4.11) into Eq. (4.9) we can get a relationship between the applied potential, the channel gap, the dielectric constant of the dielectric layer and the radii of the curvature

$$\frac{1}{R_1} = \frac{1}{R_2} - \frac{\epsilon_0 \epsilon V^2}{2\gamma_{LV}td} \quad (4.12)$$

### 4.3 Contact Angle Change

During the splitting process the height of the droplet will decrease and because of this the channel gap must be arranged so carefully that the droplet must always touch the electrodes in order to have a closed circuit. In order to arrange the channel gap, we must know how much the contact angle of the droplet will change by EWOD in the channel system. We know that the externally applied potential  $V$  in Eq. (4.12) is the voltage across the dielectric layer on the bottom wall. In the systems where we use a microchannel to split the droplet, the total voltage drop is the total of the voltage drop across the dielectric layer on the bottom wall, the voltage drop across the dielectric layer on the top wall and the voltage drop across the droplet. But here we neglect the electric resistance of the water droplet compared to that of the dielectric layers. Sung Kwon Cho and his co-workers [13] considered 2 different channel systems in order to see how the voltage drops are seen across the dielectric layers. For channel I, they coated the top layer with a 200 Angstrom Teflon layer and they coated the bottom layer with a 200 Angstrom Teflon and 1000 Angstrom Silicon dioxide layer.

For channel II, they used 200 Angstrom Teflon layer and 1000 Angstrom Silicon dioxide layer for both top and bottom electrodes. When they applied total 25 V for the first channel

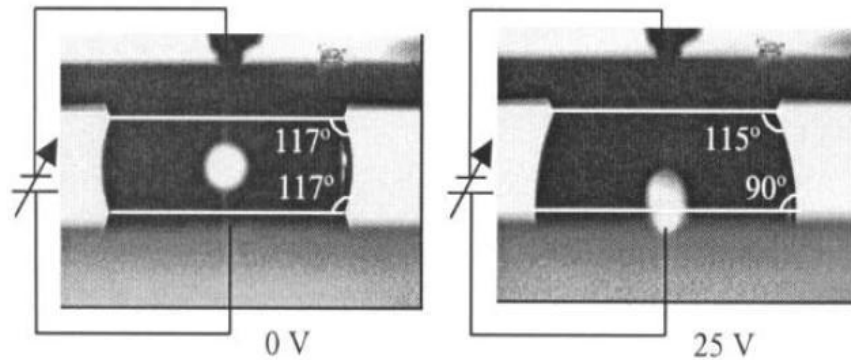


Figure 4.4: Channel I System, [14]

system, the contact angle on the top wall changed from  $117^\circ$  to  $115^\circ$  but on the bottom wall the contact angle changed from  $117^\circ$  to  $90^\circ$ . From this we can conclude that the voltage drop across the dielectric layer on the bottom wall is the total voltage drop because the voltage drop across the dielectric layer on the top wall is negligible. Fig. (4.4) shows the contact angle change on both top and bottom wall with an applied 25 V. When a 100 V is applied for the second channel system, the contact angle on both top and bottom walls changed from  $117^\circ$  to  $86^\circ$ . It means that the total voltage applied is shared equally in the top and the bottom dielectric layers. Fig. (4.5) shows the contact angle change on both top and bottom walls with an applied 100 V. From the results above we can conclude that we can split the droplet more easily by using Channel I system.

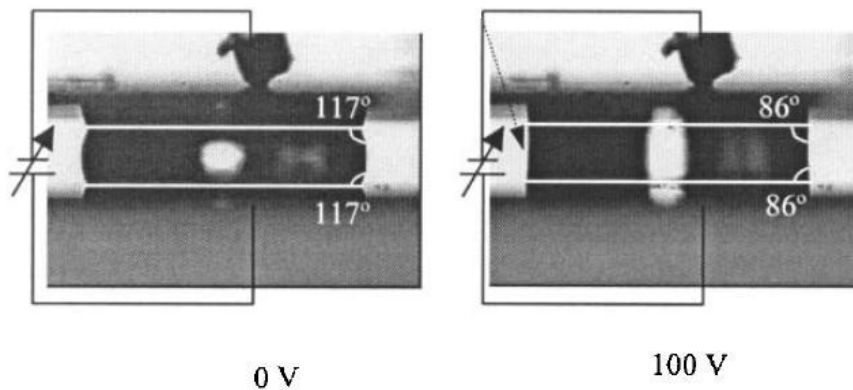


Figure 4.5: Channel II System, [14]

#### 4.4 Optimizing the Channel Gap

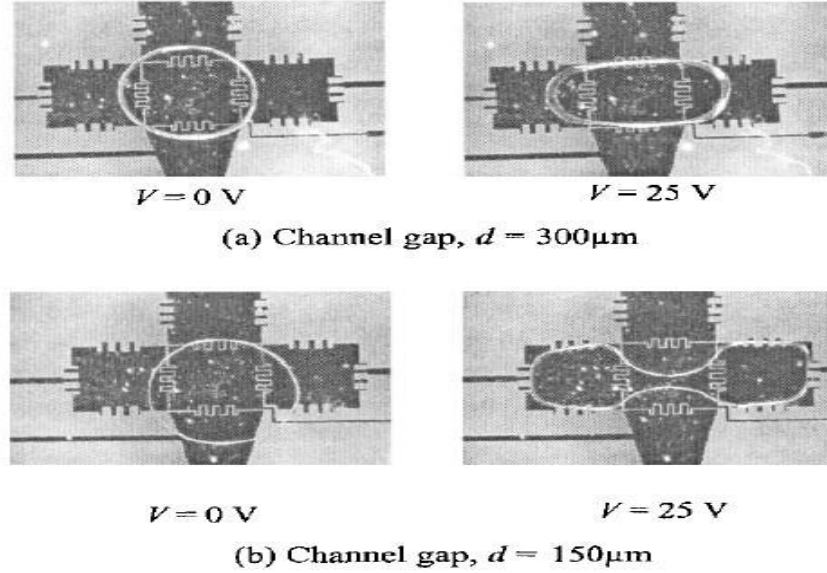


Figure 4.6: Optimizing the channel gap to have a reliable splitting, [13]

When a droplet is squeezed in a microchannel, contact angles on the top and bottom layers are almost equal to  $120^\circ$ . As explained before, contact angle saturates at about  $80^\circ$ . So, the contact angle change on the bottom layer must be smaller than  $40^\circ$ . ( $\theta_{b2}|_{V=0} - \theta_{b2} < 40^\circ$ ) Also, we want to split the droplet with a low external applied potential. If we make the calculation based on the values  $\theta_{b2}|_{V=0} = 120^\circ$ ,  $\theta_{b2} = 80^\circ$ , and the applied voltage 25 V we can conclude that the required gap for a successful splitting should be smaller than 0.15 mm. Here it was assumed that  $R_2 = 0.5 \text{ mm}$  and the splitting occurs when  $R_1$  becomes half size of the control electrode.

#### Conclusion

After all observations and calculations, we see that increasing of externally applied potential helps us split the droplet. Similarly, small gap size helps the splitting process. We have also seen that, if the channel gap size is too large compared to the droplet size, it becomes impossible to split the the droplet.

## Chapter 5

## CALCULATION OF ELECTROSTATIC FORCES AND CAPACITIVE ENERGIES FOR AN EWOD-ACTUATED DROPLET

In this section, we calculated electrostatic forces and capacitive energies on a droplet which is actuated by using EWOD configuration. We can actuate a droplet by using EWOD mechanism. To do that, let us put the droplet on a substrate containing electrodes beneath it, as in Fig. (5.1). If we apply a potential to the electrodes on one side of the droplet, charges on solid/liquid contact will be modified at the interface [15]. According to the Lippmann equation, Eq. (4.3), contact angle of the droplet which is on the energized electrodes side, will decrease and actuation towards this side will start.

### *Theoretical Calculation of Net Force*

Let us consider a droplet of height  $h$ , and length  $L$  in a microchannel which is coated with dielectric layers. The thickness of the dielectric layer is  $d_l$  on the lower electrode and  $d_u$  on the upper electrode. The dielectric constant of dielectric layer is  $\varepsilon_l$  on the lower electrode and  $\varepsilon_u$  on the upper electrode. We consider here that the droplet is situated between a grounded lower electrode and an electrode with an applied  $V_a$  potential on the upper advancing face of the droplet and a grounded electrode on the upper receding face of the droplet as seen in Fig. (5.1).

By considering a displacement of the droplet to the right by distance  $x$ , we can now write the total capacitive energy of the system;

$$U = \frac{1}{2}C_l L V_d^2 + \frac{1}{2}C_u \left(x + \frac{L}{2}\right) (V_a - V_d)^2 + \frac{1}{2}C_u \left(\frac{L}{2} - x\right) (-V_d)^2 \quad (5.1)$$

where  $V_d$  is the potential on the droplet,  $C_u$  and  $C_l$  are the capacitances (per unit length) of upper and lower coatings. We can find the droplet voltage  $V_d$  by minimizing the total energy with respect to  $V_d$ ,

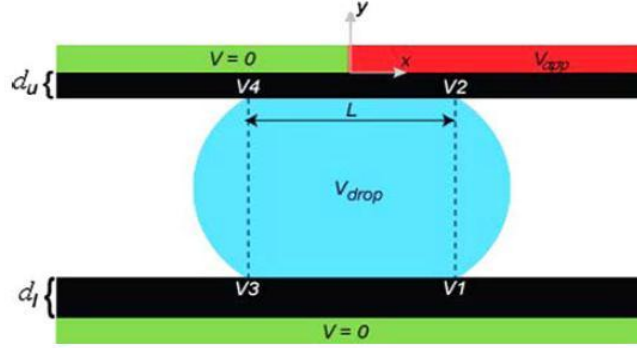


Figure 5.1: Conducting droplet in EWOD configuration, [16]

$$\frac{dU}{dV_d} = C_l L V_d - C_u \left( x + \frac{L}{2} \right) (V_a - V_d) + C_u \left( \frac{L}{2} - x \right) V_d$$

On the equation above we have a form like  $Q = C_1 V_1 + C_2 V_2 + C_3 V_3 + C_4 V_4$  and because the droplet is insulated the net charge must be zero. So, we can write;

$$\begin{aligned} 0 &= C_l L V_d + C_u L \left( \frac{x}{L} + \frac{1}{2} \right) V_d - C_u L \left( \frac{x}{L} + \frac{1}{2} \right) V_a + C_u L \left( \frac{1}{2} - \frac{x}{L} \right) V_d \\ 0 &= V_d \left[ C_l L + C_u L \left( \frac{x}{L} + \frac{1}{2} \right) + C_u L \left( \frac{1}{2} - \frac{x}{L} \right) \right] - C_u L \left( \frac{x}{L} + \frac{1}{2} \right) V_a \\ V_d &= \frac{C_u L \left( \frac{x}{L} + \frac{1}{2} \right) V_a}{L \left[ C_l + C_u \left( \frac{x}{L} + \frac{1}{2} + \frac{1}{2} - \frac{x}{L} \right) \right]} \\ V_d &= \frac{C_u V_a}{C_u + C_l} \left( \frac{x}{L} + \frac{1}{2} \right) \end{aligned} \quad (5.2)$$

We can see that when  $C_l \gg C_u$  the droplet potential is zero but when  $C_u \gg C_l$  the voltage reduces to,

$$V_d = V_a \left( \frac{x}{L} + \frac{1}{2} \right) \quad (5.3)$$

If we differentiate the total energy with respect to  $x$ , we can find the net force on the droplet in the  $x$ -direction



$$\begin{aligned}
 F_x &= \frac{dU}{dx} = C_l L V_d \frac{dV_d}{dx} - C_u \left( x + \frac{L}{2} \right) (V_a - V_d) \frac{dV_d}{dx} + \frac{C_u}{2} (V_a - V_d)^2 \\
 &\quad + C_u \left( \frac{L}{2} - x \right) V_d \frac{dV_d}{dx} - \frac{C_u}{2} V_d^2 \\
 &= C_l L V_d \frac{dV_d}{dx} - C_u \left( x + \frac{L}{2} \right) V_a \frac{dV_d}{dx} + C_u \left( x + \frac{L}{2} \right) V_d \frac{dV_d}{dx} + \frac{C_u}{2} V_a^2 \\
 &\quad + \frac{C_u}{2} V_d^2 - C_u V_a V_d + C_u \left( \frac{L}{2} - x \right) V_d \frac{dV_d}{dx} - \frac{C_u}{2} V_d^2 \\
 F_x &= C_l L V_d \frac{dV_d}{dx} - C_u \left( x + \frac{L}{2} \right) V_a \frac{dV_d}{dx} + C_u L V_d \frac{dV_d}{dx} + \frac{C_u}{2} V_a^2 - C_u V_a V_d
 \end{aligned}$$

We know from Eq. (5.2) that  $V_d = \frac{C_u V_a}{C_u + C_l} \left( \frac{x}{L} + \frac{1}{2} \right)$ . So x-derivative of droplet potential  $\frac{dV_d}{dx} = \frac{C_u V_a}{L(C_u + C_l)}$ . Substituting these equations in the force equation above we get;

$$\begin{aligned}
 F_x &= C_l L \frac{C_u^2 V_a^2}{(C_u + C_l)^2} \left( \frac{x}{L} + \frac{1}{2} \right) \frac{1}{L} - C_u^2 V_a^2 \left( x + \frac{L}{2} \right) \frac{1}{L(C_u + C_l)} \\
 &\quad + \frac{C_u^3 V_a^2}{(C_u + C_l)^2} \left( \frac{x}{L} + \frac{1}{2} \right) L \frac{1}{L} + \frac{C_u}{2} V_a^2 - \frac{C_u^2 V_a^2}{C_u + C_l} \left( \frac{x}{L} + \frac{1}{2} \right) \\
 &= C_l \frac{C_u^2 V_a^2}{(C_u + C_l)^2} \left( \frac{x}{L} + \frac{1}{2} \right) - \frac{2C_u^2 V_a^2}{C_u + C_l} \left( \frac{x}{L} + \frac{1}{2} \right) + \frac{C_u^3 V_a^2}{(C_u + C_l)^2} \left( \frac{x}{L} + \frac{1}{2} \right) + \frac{C_u}{2} V_a^2 \\
 &= \frac{C_u^2 V_a^2}{(C_u + C_l)^2} \left( \frac{x}{L} + \frac{1}{2} \right) (C_u + C_l) - \frac{2C_u^2 V_a^2}{C_u + C_l} \left( \frac{x}{L} + \frac{1}{2} \right) + \frac{C_u V_a^2}{2} \left( \frac{C_u + C_l}{C_u + C_l} \right) \\
 &= \frac{C_u^2 V_a^2}{(C_u + C_l)} \left( \frac{x}{L} + \frac{1}{2} \right) - \frac{2C_u^2 V_a^2}{C_u + C_l} \left( \frac{x}{L} + \frac{1}{2} \right) + \frac{C_u V_a^2}{2} \left( \frac{C_u + C_l}{C_u + C_l} \right) \\
 &= \frac{C_u V_a^2}{2} \left( \frac{C_u + C_l}{C_u + C_l} \right) - \frac{C_u^2 V_a^2}{C_u + C_l} \left( \frac{x}{L} + \frac{1}{2} \right) \frac{2}{2} \\
 &= \frac{1}{2} \frac{C_u V_a^2}{C_u + C_l} \left( C_u + C_l - 2C_u \frac{x}{L} - C_u \right) \\
 F_x &= \frac{1}{2} \frac{C_u V_a^2}{C_u + C_l} \left( C_l - 2C_u \frac{x}{L} \right) \tag{5.4}
 \end{aligned}$$

We can see that when the droplet is situated at center ( $x=0$ ), the force reduces to;

$$F_x = \frac{1}{2} \frac{C_u C_l V_a^2}{C_u + C_l} \tag{5.5}$$

The equation above is equal to the total capacitive energy per unit area when two dielectric layers placed at a voltage  $V_a$  are connected in series with capacitances  $C_u$ , and  $C_l$ .

If  $C_l$  goes to infinity in Eq. (5.4), the force becomes;

$$F_x = \frac{1}{2} C_u V_a^2 \tag{5.6}$$

which is independent of position  $x$ . When  $C_l$  goes to zero, the force becomes;

$$F_x = -\frac{C_u V_a^2}{L} x \tag{5.7}$$

When the capacitances of dielectric layers on both upper and lower electrodes are equal  $C_u = C_l = C$ , the force becomes

$$F_x = \frac{1}{2} \frac{C V_a^2}{2C} \left( C - 2C \frac{x}{L} \right) \tag{5.8}$$

$$F_x = \frac{C V_a^2}{4} \left( 1 - 2 \frac{x}{L} \right)$$

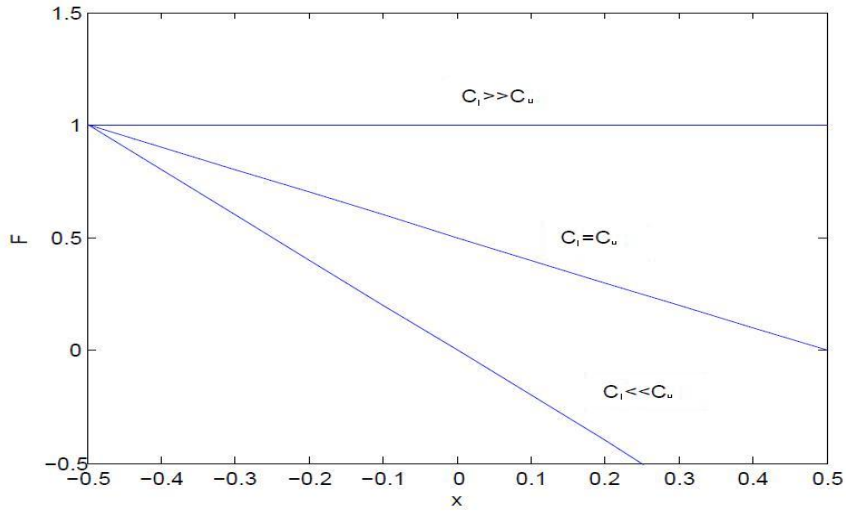


Figure 5.2: Forces acting on the droplet when  $C_l \ll C_u$ ,  $C_l = C_u$ , and  $C_l \gg C_u$

As we have seen before, when  $C_l \gg C_u$ , the droplet potential becomes zero ( $V_d = 0$ ). Then the energy of the system from Eq. (5.1) becomes;

$$U = \frac{1}{2}C_u \left(x + \frac{L}{2}\right) V_a^2 \quad (5.9)$$

When the capacitances of dielectric layers on both upper and lower electrodes are equal  $C_u = C_l = C$ , the droplet potential from Eq. (5.2) becomes

$$V_d = \frac{V_a}{2} \left(\frac{x}{L} + \frac{1}{2}\right) \quad (5.10)$$

So, the total energy of the system U becomes;

$$\begin{aligned} U &= \frac{1}{2}CLV_d^2 + \frac{1}{2}C \left(x + \frac{L}{2}\right) V_a^2 + \frac{1}{2}C \left(x + \frac{L}{2}\right) V_d^2 - C \left(x + \frac{L}{2}\right) V_a V_d + \frac{C}{2} \left(\frac{L}{2} - x\right) V_d^2 \\ &= \frac{1}{2}CLV_d^2 + \frac{1}{2}C \left(x + \frac{L}{2}\right) V_a^2 + \frac{1}{2}CV_d^2 L - C \left(x + \frac{L}{2}\right) V_a V_d \\ &= CLV_d^2 + \frac{1}{2}C \left(x + \frac{L}{2}\right) V_a^2 - C \left(x + \frac{L}{2}\right) V_a V_d \\ &= CL \frac{V_a^2}{4} \left(\frac{x}{L} + \frac{1}{2}\right)^2 + \frac{1}{2}CV_a^2 \left(x + \frac{L}{2}\right) - \frac{CV_a^2}{2} \left(\frac{x}{L} + \frac{1}{2}\right) \left(x + \frac{L}{2}\right) \\ &= CL \frac{V_a^2}{4} \left(\frac{x}{L} + \frac{1}{2}\right)^2 + \frac{1}{2}CV_a^2 L \left(\frac{x}{L} + \frac{1}{2}\right) - \frac{CV_a^2}{2} L \left(\frac{x}{L} + \frac{1}{2}\right)^2 \\ &= \frac{1}{2}CV_a^2 L \left(\frac{x}{L} + \frac{1}{2}\right) - \frac{CV_a^2}{4} L \left(\frac{x}{L} + \frac{1}{2}\right)^2 \\ &= \frac{1}{2}CV_a^2 L \left(\frac{x}{L} + \frac{1}{2}\right) \left(1 - \frac{1}{2} \left(\frac{x}{L} + \frac{1}{2}\right)\right) \\ U &= \frac{1}{2}CV_a^2 L \left(\frac{x}{L} + \frac{1}{2}\right) \left(\frac{3}{4} - \frac{x}{2L}\right) \quad (5.11) \end{aligned}$$

Now we can see how the total energy of the system changes when  $C_u \gg C_l$ . From Eq. (5.3) droplet potential has the value of  $V_d = V_a \left(\frac{x}{L} + \frac{1}{2}\right)$ . So, when we substitute this equation in Eq. (5.1) we get,

$$\begin{aligned} U &= \frac{1}{2}C_l V_a^2 L \left(\frac{x}{L} + \frac{1}{2}\right)^2 + \frac{1}{2}C_u \left(x + \frac{L}{2}\right) V_a^2 + \frac{1}{2}C_u \left(x + \frac{L}{2}\right) V_d^2 - C_u \left(x + \frac{L}{2}\right) V_a V_d \\ &\quad + \frac{C_u}{2} \left(\frac{L}{2} - x\right) V_d^2 \\ &= \frac{1}{2}C_l V_a^2 L \left(\frac{x}{L} + \frac{1}{2}\right)^2 + \frac{1}{2}C_u \left(x + \frac{L}{2}\right) V_a^2 + \frac{1}{2}C_u V_d^2 L - C_u \left(x + \frac{L}{2}\right) V_a V_d \end{aligned}$$

$$\begin{aligned}
 &= \frac{1}{2}C_l V_a^2 L \left(\frac{x}{L} + \frac{1}{2}\right)^2 + \frac{1}{2}C_u \left(x + \frac{L}{2}\right) V_a^2 + \frac{1}{2}C_u V_a^2 L \left(\frac{x}{L} + \frac{1}{2}\right)^2 \\
 &\quad - C_u \left(x + \frac{L}{2}\right) V_a^2 \left(\frac{x}{L} + \frac{1}{2}\right) \\
 &= \frac{1}{2}C_l V_a^2 L \left(\frac{x}{L} + \frac{1}{2}\right)^2 + \frac{1}{2}C_u V_a^2 L \left(\frac{x}{L} + \frac{1}{2}\right) + \frac{1}{2}C_u V_a^2 L \left(\frac{x}{L} + \frac{1}{2}\right)^2 \\
 &\quad - C_u V_a^2 L \left(\frac{x}{L} + \frac{1}{2}\right)^2 \\
 &= \frac{1}{2}C_l V_a^2 L \left(\frac{x}{L} + \frac{1}{2}\right)^2 + \frac{1}{2}C_u V_a^2 L \left(\frac{x}{L} + \frac{1}{2}\right) - \frac{1}{2}C_u V_a^2 L \left(\frac{x}{L} + \frac{1}{2}\right)^2 \\
 &= \frac{1}{2}V_a^2 L \left(\frac{x}{L} + \frac{1}{2}\right)^2 (C_l - C_u) + \frac{1}{2}C_u V_a^2 L \left(\frac{x}{L} + \frac{1}{2}\right)
 \end{aligned}$$

Since  $C_u \gg C_l$ , we can neglect  $C_l$  in the first term of equation above. Then we get;

$$\begin{aligned}
 U &= \frac{1}{2}C_u V_a^2 L \left(\frac{x}{L} + \frac{1}{2}\right) - \frac{1}{2}C_u V_a^2 L \left(\frac{x}{L} + \frac{1}{2}\right)^2 \\
 &= \frac{1}{2}C_u V_a^2 L \left(\frac{x}{L} + \frac{1}{2}\right) \left(1 - \frac{x}{L} - \frac{1}{2}\right) \\
 &= \frac{1}{2}C_u V_a^2 L \left(\frac{x}{L} + \frac{1}{2}\right) \left(\frac{1}{2} - \frac{x}{L}\right) \\
 U &= \frac{1}{2}C_u V_a^2 L \left(\frac{1}{4} - \frac{x^2}{L^2}\right)
 \end{aligned} \tag{5.12}$$

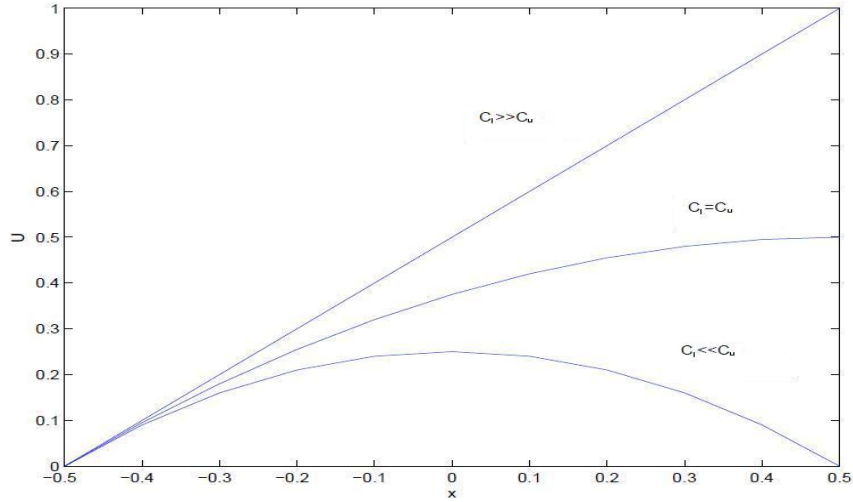


Figure 5.3: Capacitive energies for the droplet when  $C_l \ll C_u$ ,  $C_l = C_u$ , and  $C_l \gg C_u$

We have seen that, when the capacitance of the lower dielectric layer,  $C_l$ , is very large, the force acting on the droplet is constant. However, when  $C_l$  is low enough the force decreases linearly as the droplet moves. Similarly, if the capacitance of the lower and upper layers are the same, we again see that the force decreases as the droplet moves. In Fig. (5.3) we can see that, when capacitance of the lower layer is much larger than the capacitance of the upper layer, capacitive energy increases linearly according to Eq. (5.9) as the droplet moves. If we consider capacitances of upper and lower dielectrics equal, the capacitive energy changes according to Eq. (5.11) and we can also see that, capacitive energy goes to zero at two different points,  $x=-0.5$  and  $x=1.5$ . When the capacitance of the upper layer is much larger than the capacitance of the lower layer, the capacitive energy has a maximum point at  $x=0$  and becomes zero at  $x=-0.5$  and  $x=0.5$ .

## Chapter 6

**CHARGE-RELATED WETTING PHENOMENA**

In this section, we have examined 3 cases of wetting phenomena, as seen in Fig. (6.1). In each case, the force acting on the liquid-droplet interface has been calculated. In the first case, case a) in Fig. (6.1), the droplet is situated on a substrate and the potential is kept constant on the substrate. For the second case, case b) in Fig. (6.1), there is no external applied potential but constant charge density on the droplet-substrate surface and another constant charge density on the liquid-substrate surface. For the last case, case c) in Fig. (6.1), there is a dielectric layer situated on the substrate and constant potential  $V$  is applied. All the aforementioned cases are called *charge-related wetting phenomena*.

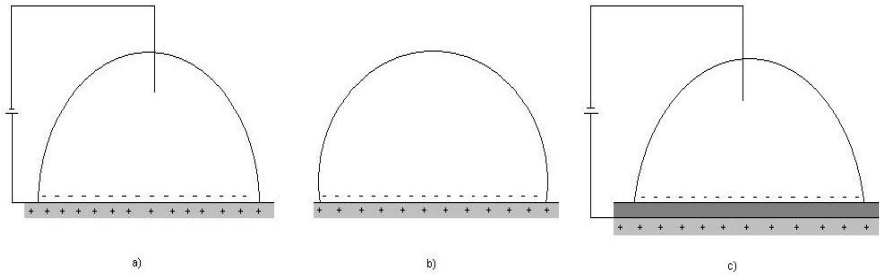


Figure 6.1: Charge Related Wetting Phenomena

Let us consider a two-dimensional droplet which is in equilibrium on a substrate and immersed in a fluid. In order to find the electrostatic force acting on the droplet-liquid interface, we can define two surfaces [17];  $\sum_1 = S_{12} \cup S_{13} \cup S_{1\infty}$ , and  $\sum_2 = S_{21} \cup S_{22} \cup S_{23} \cup S_{2\infty}$ . Here  $\sum_1$  encloses the droplet region and  $\sum_2$  encloses the fluid region. Indices 1, 2, and 3 indicate the variables associated with droplet, fluid, and substrate respectively. Also double indices in  $S_{ij}$  indicate the surface which is in the  $i^{th}$  medium facing the  $j^{th}$  medium.  $S_{1\infty}$ , and  $S_{2\infty}$  indicate the surfaces which are perpendicular to the substrate and situated at a large distance from three phase contact line, TCL.

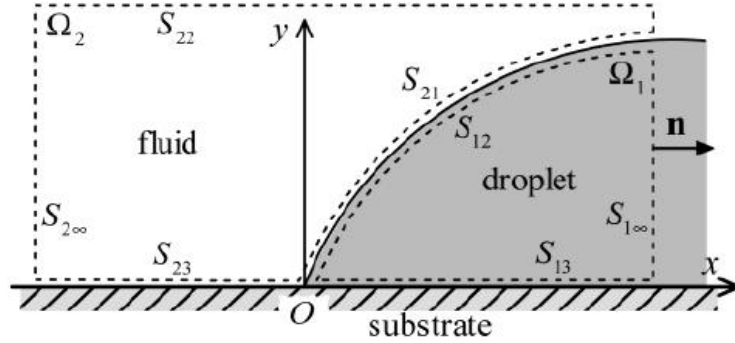


Figure 6.2: Control Surfaces of the System, [17]

We can find the electrostatic force acting on the droplet-fluid interface by integrating the stress acting on the droplet-fluid interface [20]:

$$\mathbf{F} = - \int_{S_{12}+S_{21}} \mathbf{T} \cdot \mathbf{n} dS \quad (6.1)$$

where  $\mathbf{T} = -(\Pi + (1/2)\epsilon E^2)\mathbf{I} + \epsilon \mathbf{E}\mathbf{E}$  is the sum of Maxwell stress tensor and osmotic pressure tensor ( $\Pi$ ),  $\mathbf{n}$  is the outward unit normal vector at the surfaces,  $\mathbf{E}$  is the electric field,  $\epsilon$  is the electric permittivity, and  $\mathbf{I}$  is the second order isotropic tensor.

We assume that the electrical double layer satisfies Poisson-Boltzmann equation (Eq. (3.5)). The osmotic pressure is given by [22],

$$\Pi = 2n_0 kT [\cosh(\beta\varphi) - 1]$$

where  $\beta = ez/kT$ .

By using the mechanical equilibrium condition, we can simplify the integral in Eq. (6.1). Mechanical equilibrium condition states that [21],

$$\int_{\Sigma} \mathbf{T} \cdot \mathbf{n} dS = \int_{\Sigma} \left[ - \left( \Pi + \frac{1}{2} \epsilon E^2 \right) \mathbf{I} + \epsilon \mathbf{E}\mathbf{E} \right] \cdot \mathbf{n} dS = 0 \quad (6.2)$$

### 6.1 Constant Potential Case (Case I)

In this case, the potential is constant ( $\varphi = V$ ) on the substrate surface ( $S_{13}$ , and  $S_{23}$ ). We can separate the force acting on the liquid-droplet interface into two parts, the force acting on the droplet side ( $\mathbf{F}_1$ ) and the force acting on the liquid side ( $\mathbf{F}_2$ ).

$$\mathbf{F} = \mathbf{F}_1 + \mathbf{F}_2 = - \int_{S_{12}} \mathbf{T} \cdot \mathbf{n} dS - \int_{S_{21}} \mathbf{T} \cdot \mathbf{n} dS \quad (6.3)$$

Now, we can examine  $(\mathbf{F}_1)$  and  $(\mathbf{F}_2)$  separately by using Eq. (6.2),

$$\begin{aligned} \int_{S_{12}+S_{13}+S_{1\infty}} \mathbf{T} \cdot \mathbf{n} dS &= \int_{S_{12}} \mathbf{T} \cdot \mathbf{n} dS + \int_{S_{13}} \mathbf{T} \cdot \mathbf{n} dS + \int_{S_{1\infty}} \mathbf{T} \cdot \mathbf{n} dS = 0 \\ - \int_{S_{12}} \mathbf{T} \cdot \mathbf{n} dS &= \int_{S_{13}} \mathbf{T} \cdot \mathbf{n} dS + \int_{S_{1\infty}} \mathbf{T} \cdot \mathbf{n} dS \end{aligned}$$

We can also write;

$$\begin{aligned} \int_{S_{21}+S_{22}+S_{23}+S_{2\infty}} \mathbf{T} \cdot \mathbf{n} dS &= \int_{S_{21}} \mathbf{T} \cdot \mathbf{n} dS + \int_{S_{22}} \mathbf{T} \cdot \mathbf{n} dS + \int_{S_{23}} \mathbf{T} \cdot \mathbf{n} dS \\ &\quad + \int_{S_{2\infty}} \mathbf{T} \cdot \mathbf{n} dS = 0 \end{aligned}$$

$$- \int_{S_{21}} \mathbf{T} \cdot \mathbf{n} dS = \int_{S_{22}} \mathbf{T} \cdot \mathbf{n} dS + \int_{S_{23}} \mathbf{T} \cdot \mathbf{n} dS + \int_{S_{2\infty}} \mathbf{T} \cdot \mathbf{n} dS$$

Finally;

$$\mathbf{F}_1 + \mathbf{F}_2 = \int_{S_{13}+S_{1\infty}} \mathbf{T} \cdot \mathbf{n} dS + \int_{S_{22}+S_{23}+S_{2\infty}} \mathbf{T} \cdot \mathbf{n} dS$$

Now, let's consider these two components separately:

$$\begin{aligned} \mathbf{F}_1 &= \int_{S_{1\infty}} \left[ - \left( \Pi + \frac{1}{2} \epsilon_1 E^2 \right) \mathbf{n} + \epsilon_1 (\mathbf{n} \cdot \mathbf{E}) \mathbf{E} \right] dS \\ &\quad + \int_{S_{13}} \left[ - \left( \Pi + \frac{1}{2} \epsilon_1 E^2 \right) \mathbf{n} + \epsilon_1 (\mathbf{n} \cdot \mathbf{E}) \mathbf{E} \right] dS \end{aligned}$$

At large distances from TCL ( $S_{1\infty}$ ,  $S_{2\infty}$ ), the electric field is not normal to the control surfaces which means  $\mathbf{E} \cdot \mathbf{n}|_{S_{1\infty}} = 0$ . Therefore,  $\mathbf{F}_1$  becomes,

$$\begin{aligned} \mathbf{F}_1 &= - \int_{S_{1\infty}} \left( \Pi + \frac{1}{2} \epsilon_1 E^2 \right) \mathbf{n} dS \\ &\quad + \int_{S_{13}} \left[ - \left( \Pi + \frac{1}{2} \epsilon_1 E^2 \right) \mathbf{n} + \epsilon_1 (\mathbf{n} \cdot \mathbf{E}) \mathbf{E} \right] dS \end{aligned} \quad (6.4)$$



Wetting tension is given by  $W_{el} = -\mathbf{F} \cdot \mathbf{e}_x$ . So, we are interested in the horizontal component of  $\mathbf{F}_1$ , that is,  $f_{1x} = \mathbf{F}_1 \cdot \mathbf{e}_x$ .

$$f_{1x}^{(1)} = - \int_{S_{1\infty}} \left( \Pi + \frac{1}{2} \epsilon_1 E^2 \right) \mathbf{n} \cdot \mathbf{e}_x dS \\ + \int_{S_{13}} \left[ - \left( \Pi + \frac{1}{2} \epsilon_1 E^2 \right) \mathbf{n} \cdot \mathbf{e}_x + \epsilon_1 (\mathbf{n} \cdot \mathbf{E}) \mathbf{E} \cdot \mathbf{e}_x \right] dS$$

We know that on the horizontal substrate surface normal vector  $\mathbf{n}$  is perpendicular to the normal vector  $\mathbf{e}_x$  which means  $\mathbf{n} \cdot \mathbf{e}_x|_{S_{13}} = 0$ . Then, we can write,

$$f_{1x}^{(1)} = - \int_{S_{1\infty}} \left( \Pi + \frac{1}{2} \epsilon_1 E^2 \right) \mathbf{n} \cdot \mathbf{e}_x dS + \int_{S_{13}} \epsilon_1 (\mathbf{n} \cdot \mathbf{E}) \mathbf{E} \cdot \mathbf{e}_x dS \quad (6.5)$$

In case I, the electrostatic potential is constant on the horizontal surface ( $\varphi|_{S_{13}} = V$ ) which means  $\mathbf{E} \cdot \mathbf{e}_x|_{S_{13}} = -(d\varphi/dx)|_{S_{13}} = 0$ . Because of this reason, the second integral in Eq. (6.5) vanishes. As a result we have,

$$f_{1x}^{(1)} = - \int_{S_{1\infty}} \left( \Pi + \frac{1}{2} \epsilon_1 E^2 \right) \mathbf{n} \cdot \mathbf{e}_x dS \quad (6.6)$$

Eq. (6.6) corresponds to the free energy of the plane electrical double layer and it is [17],

$$f_{1x}^{(1)} = -8 \frac{n_{1b} kT}{K_1} \left[ \cosh \left( \frac{\beta V}{2} \right) - 1 \right] \quad (6.7)$$

We can calculate the force acting on the fluid side ( $\mathbf{F}_2$ ) and then calculate  $f_{2x}^{(1)}$  following the same procedure. Consequently,

$$f_{2x}^{(1)} = 8 \frac{n_{2b} kT}{K_2} \left[ \cosh \left( \frac{\beta V}{2} \right) - 1 \right] \quad (6.8)$$

Finally, the wetting tension  $W_{el}^{(1)} = -f_{1x}^{(1)} - f_{2x}^{(1)}$  becomes,

$$W_{el}^{(1)} = 8kT \left( \frac{n_{1b}}{K_1} - \frac{n_{2b}}{K_2} \right) \left[ \cosh \left( \frac{\beta V}{2} \right) - 1 \right] \quad (6.9)$$

## 6.2 Constant Charge Case (Case II)

In case II, we keep the surface charge densities constant on the surfaces  $S_{13}$ , and  $S_{23}$ . Let the surface charge density on  $S_{13}$  be  $\sigma_1$  and the surface charge density on  $S_{23}$  be  $\sigma_2$ . Again, we can separate the forces acting on the droplet-fluid interface and examine them separately.

$$\mathbf{F}_1 + \mathbf{F}_2 = \int_{S_{13}+S_{1\infty}} \mathbf{T} \cdot \mathbf{n} dS + \int_{S_{22}+S_{23}+S_{2\infty}} \mathbf{T} \cdot \mathbf{n} dS \quad (6.10)$$

At large distances from TCL ( $S_{1\infty}$ ,  $S_{2\infty}$ ) we remember that  $\mathbf{E} \cdot \mathbf{n}|_{S_{1\infty}, S_{2\infty}} = 0$  and at horizontal surfaces  $\mathbf{n} \cdot \mathbf{e}_x|_{S_{13}, S_{23}} = 0$ . Unlike in Eq. (6.6) the second integral will not vanish in this case and the force acting on  $S_{12}$  will be,

$$f_{1x}^{(2)} = - \int_{S_{1\infty}} \left( \Pi + \frac{1}{2} \epsilon_1 E^2 \right) \mathbf{n} \cdot \mathbf{e}_x dS + \int_{S_{13}} \epsilon_1 (\mathbf{n} \cdot \mathbf{E}) \mathbf{E} \cdot \mathbf{e}_x dS \quad (6.11)$$

The first integral will be very similar to Eq. (6.7) except the potential term  $V$ . We know that  $\epsilon_1 \mathbf{E} \cdot \mathbf{n}|_{S_{13}} = -\sigma_1$  and  $\mathbf{E} \cdot \mathbf{e}_x|_{S_{13}} = -(d\varphi/dx)|_{S_{13}}$ . So, for the second integral we can write,

$$\int_{S_{13}} \epsilon_1 (\mathbf{n} \cdot \mathbf{E}) \mathbf{E} \cdot \mathbf{e}_x dS = \sigma_1 \int_0^\infty \frac{d\varphi}{dx} dx = \sigma_1 (\varphi_{1\infty} - \varphi_0)$$

where  $\varphi_0$  is the electrostatic potential at TCL, and  $\varphi_{1\infty}$  is the electrostatic potential far from TCL. Now, we can write the force acting on  $S_{12}$  as,

$$f_{1x}^{(2)} = -8 \frac{n_{1b} kT}{K_1} \left[ \cosh \left( \frac{\beta \varphi_{1\infty}}{2} \right) - 1 \right] + \sigma_1 (\varphi_{1\infty} - \varphi_0)$$

The force acting on  $S_{21}$ ,  $f_{2x}^{(2)}$ , can be calculated with a similar way. Consequently,

$$f_{2x}^{(2)} = 8 \frac{n_{2b} kT}{K_2} \left[ \cosh \left( \frac{\beta \varphi_{2\infty}}{2} \right) - 1 \right] + \sigma_2 (\varphi_0 - \varphi_{2\infty})$$

Finally, the wetting tension  $W_{el}^{(2)} = -f_{1x}^{(2)} - f_{2x}^{(2)}$  becomes,

$$\begin{aligned} W_{el}^{(2)} = & \left( \frac{8n_{1b} kT}{K_1} \left[ \cosh \left( \frac{\beta \varphi_{1\infty}}{2} \right) - 1 \right] - \sigma_1 \varphi_{1\infty} \right) \\ & - \left( \frac{8n_{2b} kT}{K_2} \left[ \cosh \left( \frac{\beta \varphi_{2\infty}}{2} \right) - 1 \right] - \sigma_2 \varphi_{2\infty} \right) + (\sigma_1 - \sigma_2) \varphi_0 \end{aligned} \quad (6.12)$$

As we can see, the results of Case I and Case II differ by an extra term. The first and the second terms in Case II represent the electrostatic free energy of the double layer which has constant charge density. However, the last term is due to the Coulombic interaction near TCL.

### 6.3 Electrowetting on Dielectrics (EWOD) Case (Case III)

EWOD mechanism has drawn much attention due to its applications on controlling droplets. By using this mechanism, droplets having very small volumes can be controlled with low power consumption [18, 19].

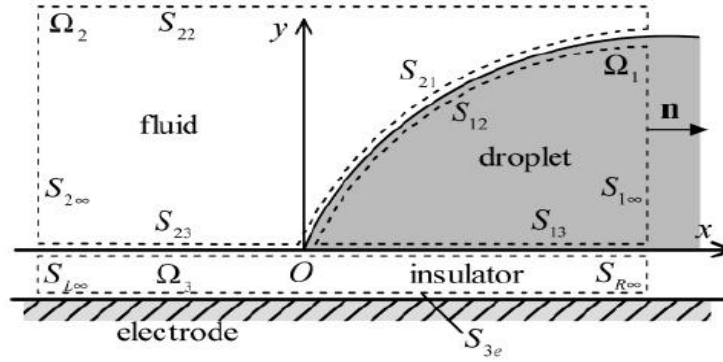


Figure 6.3: Control Surfaces of EWOD System, [17]

The difference of this case from case I is that there is a thin dielectric layer between droplet and the substrate as in Fig. (6.3). We know from previous cases that the force acting on the liquid-droplet interface can be written as,

$$\mathbf{F}_1 + \mathbf{F}_2 = \int_{S_{13}+S_{1\infty}} \mathbf{T} \cdot \mathbf{n} dS + \int_{S_{22}+S_{23}+S_{2\infty}} \mathbf{T} \cdot \mathbf{n} dS \quad (6.13)$$

Now, the horizontal component of the force can be written as,

$$f_x^{(3)} = \mathbf{e}_x \cdot \int_{S_{13}+S_{1\infty}} \mathbf{T} \cdot \mathbf{n} dS + \mathbf{e}_x \cdot \int_{S_{22}+S_{23}+S_{2\infty}} \mathbf{T} \cdot \mathbf{n} dS \quad (6.14)$$

From previous case, we know that,

$$\mathbf{e}_x \cdot \int_{S_{1\infty}} \mathbf{T} \cdot \mathbf{n} dS = -8 \frac{n_{1b} kT}{K_1} \left[ \cosh \left( \frac{\beta \varphi_{1\infty}}{2} \right) - 1 \right]$$

$$\mathbf{e}_x \cdot \int_{S_{2\infty}} \mathbf{T} \cdot \mathbf{n} dS = 8 \frac{n_{2b} kT}{K_2} \left[ \cosh \left( \frac{\beta \varphi_{2\infty}}{2} \right) - 1 \right]$$

Also, we can write the equation  $\mathbf{e}_x \cdot \int_{S_{13}+S_{23}} \mathbf{T} \cdot \mathbf{n} dS$  as;

$$\begin{aligned} \mathbf{e}_x \cdot \int_{S_{13}} (\Pi + (1/2)\epsilon E^2) \mathbf{n} dS + \int_{S_{13}} \epsilon (\mathbf{E} \cdot \mathbf{e}_x) \mathbf{E} \cdot \mathbf{n} dS + \mathbf{e}_x \cdot \int_{S_{23}} (\Pi + (1/2)\epsilon E^2) \mathbf{n} dS \\ + \int_{S_{23}} \epsilon (\mathbf{E} \cdot \mathbf{e}_x) \mathbf{E} \cdot \mathbf{n} dS \end{aligned}$$

On the horizontal substrate surfaces,  $\mathbf{n} \cdot \mathbf{e}_x|_{S_{13}, S_{23}} = 0$ , and consequently

$$\mathbf{e}_x \cdot \int_{S_{13}, S_{23}} (\Pi + (1/2)\epsilon E^2) \mathbf{n} dS = 0$$

Eq. (6.13) now can be written as,

$$\begin{aligned} f_x^{(3)} = -8 \frac{n_{1b} kT}{K_1} \left[ \cosh \left( \frac{\beta \varphi_{1\infty}}{2} \right) - 1 \right] + 8 \frac{n_{2b} kT}{K_2} \left[ \cosh \left( \frac{\beta \varphi_{2\infty}}{2} \right) - 1 \right] \\ + \int_{S_{13}+S_{23}} \epsilon (\mathbf{E} \cdot \mathbf{e}_x) \mathbf{E} \cdot \mathbf{n} dS \end{aligned} \quad (6.15)$$

Since  $\mathbf{n} \cdot \mathbf{e}_x|_{S_{13}, S_{23}} = 0$

$$\int_{S_{31}+S_{32}} \epsilon (\mathbf{E} \cdot \mathbf{e}_x) \mathbf{E} \cdot \mathbf{n} dS = \mathbf{e}_x \cdot \int_{S_{31}+S_{32}} \mathbf{T}' dS$$

where  $\mathbf{T}' = -\frac{1}{2}\epsilon E^2 \mathbf{n} + \epsilon \mathbf{E}(\mathbf{E} \cdot \mathbf{n})$

We know that the normal electric flux and the tangential component of electric field must be continuous; which means,

$$\epsilon \mathbf{E} \cdot \mathbf{n}|_{S_{13}, S_{23}} = -\epsilon \mathbf{E} \cdot \mathbf{n}|_{S_{31}, S_{32}}$$

$$\mathbf{E} \cdot \mathbf{e}_x|_{S_{13}, S_{23}} = -\frac{d\varphi}{dx}|_{S_{13}, S_{23}} = -\frac{d\varphi}{dx}|_{S_{31}, S_{32}} = \mathbf{E} \cdot \mathbf{e}_x|_{S_{31}, S_{32}}$$

Consequently,

$$\int_{S_{13}+S_{23}} \epsilon(\mathbf{E} \cdot \mathbf{e}_x) \mathbf{E} \cdot \mathbf{n} dS = - \int_{S_{31}+S_{32}} \epsilon(\mathbf{E} \cdot \mathbf{e}_x) \mathbf{E} \cdot \mathbf{n} dS$$

By using mechanical equilibrium condition, we can write,

$$\mathbf{e}_x \cdot \int_{S_{31}+S_{32}+S_{L\infty}+S_{R\infty}+S_{3e}} \mathbf{T}' \cdot \mathbf{n} dS = 0$$

$$\begin{aligned} \mathbf{e}_x \cdot \int_{S_{31}+S_{32}} \mathbf{T}' \cdot \mathbf{n} dS &= - \mathbf{e}_x \cdot \int_{S_{L\infty}+S_{R\infty}+S_{3e}} \mathbf{T}' \cdot \mathbf{n} dS \\ &= - \mathbf{e}_x \cdot \int_{S_{L\infty}+S_{R\infty}+S_{3e}} \left[ -\frac{1}{2} \epsilon E^2 \mathbf{n} + \epsilon \mathbf{E}(\mathbf{E} \cdot \mathbf{n}) \right] dS \end{aligned}$$

We know that  $\mathbf{E} \cdot \mathbf{n}|_{S_{R\infty}, S_{L\infty}} = 0$ , and

$$\begin{aligned} E_1 &= \frac{V - \varphi_{1\infty}}{d} \\ E_2 &= \frac{V - \varphi_{2\infty}}{d} \end{aligned}$$

We know that  $\mathbf{n} \cdot \mathbf{e}_x|_{S_{3e}} = 0$  and since the potential is constant on  $S_{3e}$  ( $\varphi|_{S_{3e}} = V$ ) there is no contribution from the surface  $S_{3e}$ . Therefore,

$$\int_{S_{L\infty}+S_{R\infty}+S_{3e}} \mathbf{e}_x \cdot (\mathbf{T}' \cdot \mathbf{n}) dS = \frac{\epsilon_3}{2d} [(V - \varphi_{1\infty})^2 - (V - \varphi_{2\infty})^2]$$

where  $\epsilon_3$  is the electric permittivity of the dielectric layer

If we substitute everything in Eq. (6.14), we get the wetting tension,

$$\begin{aligned} W_{el}^{(3)} &= - f_x^{(3)} \\ W_{el}^{(3)} &= \frac{\epsilon_3}{2d} [(V - \varphi_{1\infty})^2 - (V - \varphi_{2\infty})^2] + 8 \frac{n_{1b} kT}{K_1} \left[ \cosh \left( \frac{\beta \varphi_{1\infty}}{2} \right) - 1 \right] \\ &\quad - 8 \frac{n_{2b} kT}{K_2} \left[ \cosh \left( \frac{\beta \varphi_{2\infty}}{2} \right) - 1 \right] \end{aligned} \quad (6.16)$$

Here, the first term comes due to the dielectric layer but last two terms again represent the free energy of the double layer.

## Chapter 7

**CONCLUSION**

We have seen that contact angles of droplets behave differently on different substrates and by using some methods we have tried to explain why contact angles change as the surface changes. We have also seen that the most important parameters to split a droplet reliably are the channel gap, the applied voltage and the droplet size. If these parameters are suitably combined, the droplet can be split easily. We know that, we can actuate a droplet by using ewod configuration. We have calculated capacitive energies and electrostatic forces on an ewod-actuated droplet and seen that their results are different for different cases. These forces and energies have been examined for three different cases where  $C_l \gg C_u$ ,  $C_l \ll C_u$ , and  $C_l = C_u = C$ . The capacitive energy results are in agreement with the graph given in the paper [16]. Finally, we have seen that when a droplet is put on a substrate where we keep a constant potential, the force acting on the fluid-droplet interface gives a different result when it is put on a substrate where we keep the charge density constant or when it is put on a dielectric layer.

**BIBLIOGRAPHY**

- [1] C. Yang, U. Tartaglino, and B.N.J. Persson (2008), Nanodroplets on Rough Hydrophilic and Hydrophobic Surfaces, *Eur. Phys. J.E* 25: 139-152.
- [2] T. Young (1805), *Philos. Trans. R. Soc. London* 95, 65
- [3] J. Bico, C. Tordeux and David Quere (2001), Rough Wetting, *Europhys. Lett.* 55: 214-220.
- [4] David Quere(2002), Rough Ideas on Wetting, *Physica A* , 313: 32-46.
- [5] Altti Torkkeli (2003), Droplet Microfluidics on a Planar Surface, *VTT Publications* 504
- [6] Vaibhav Bahadur and Suresh V. Garimella (2007), Electrowetting-Based Control of Static Droplet States on Rough Surfaces *Langmuir*, 23: 4918-4924.
- [7] John David Jackson, Classical Electrodynamics, *John Wiley and Sons, Inc.*, New York (1962).
- [8] J. Theodoor G. Overbeek (1990), The Role of Energy and Entropy in the Electrical Double Layer *Colloids and Surfaces*, 51: 61-75.
- [9] David J. Griffiths, Introduction to Electrodynamics, *Prentice Hall*, New Jersey (1999).
- [10] Lippmann, M.G., (1875), Relations Entre les Phenomenes Electriques et Cappillaires *Amm. Chim. Phys*, 5: 494-549.
- [11] Verheijen, H.J.I. and Prins, M.W.J., (1999), Reversible Electrowetting and Trapping of Charge: Model and Experiments *Langmuir*, 15: 6616-6620.
- [12] Peykov, V., Quinn, A., and Ralston, J., (2000), Electrowetting: a Model for Contact Angle Saturation *Colloid Polymer Science*, 278: 789-793.

- 
- [13] Sung Kwon Cho, Hyejin Moon, Jesse Fowler, and Chang-Jin "CJ" Kim (2001), Splitting a Liquid Droplet for Electrowetting-Based Microfluidics *International Mechanical Engineering Congress and Exposition, New York*, IMECE2001/MEMS-23830.
- [14] Sung Kwon Cho, Hyejin Moon, and Chang-Jin Kim (2003), Creating, Transporting, Cutting, and Merging Liquid droplets by Electrowetting-Based Actuation for Digital Microfluidic Circuits, *Journal of Microelectromechanical Systems*, 12: 70-80
- [15] Ilju Moon, Joonwon Kim (2006), Using EWOD Actuation in a Micro Conveyor System, *Sensors and Actuators A*, 537-544
- [16] E. Baird., P. Young., K. Mohseni (2007), Electrostatic Force Calculation for an EWOD-Actuated Droplet *Microfluid Nanofluid*, 13: 635-644
- [17] Kwan Hyoung Kang, In Seok Kang, and Choung Mook Lee, (2003), Wetting Tension Due to Coulombic Interaction in Charge-Related Wetting Phenomena, *Langmuir*, 19: 5407-5412
- [18] Quillet, C., Berge, B., (2001), *Curr. Opin. Colloid Sci*, 6: 34-39,
- [19] Quinn, A., Sedev, R., Ralston, J., (2003), *J. Phys. Chem. B*, 107: 1163-1169,
- [20] Russel, W. B., Saville, D. A., Schowalter, W. R., *Colloidal Dispersions; Cambridge University Press*, Cambridge (1989)
- [21] Landau, L. D., Lifshitz, E. M., *Electrodynamics of Continuous Media*, *Pergamon Press*, Sydney (1960)
- [22] Adamson, A. W., Gast, A. P., *Physical Chemistry of Surfaces*, *John Wiley and Sons.*, New York (1997)
- [23] T. Young, *Phil. Trans. R. Soc. Lond.*, 95 (1805), 65
- [24] P. S. Laplace *Paris: Imprimerie Royale*, (1847)



- 
- [25] J. Rowlinson, B. Widom, (1982), *Molecular Theory of Capillarity*, Oxford: Oxford University Press
- [26] P. G. de Gennes, *Rev. Mod. Phys.*, 57: No:3, Part I, 827 (1985)
- [27] D. Quere, *Rep. Prog. Phys.* 68: 2495, (2005)
- [28] T. S. Chow, *J. Phys.: Condensed Matter* ,10: L445 (1998)
- [29] N. A. Patankar, *Langmuir*, 19: 1249 (2003)
- [30] W. Chen, *Langmuir*, 15: 3395 (1999)
- [31] M. Callics and D. Quere, *Soft Matter*, 1: 55 (2005)
- [32] Patankar, N. A., (2003), *Langmuir*, 19: 1249
- [33] Kimi J., Kim, C. J., (2002), *Proc. IEEE Conf. MEMS. Las Vegas*, 479-482
- [34] Onda, T., Siniuchi, S., Satoh, N., Tsujii, K., *Langmuir*, 12: 2125 (1996)
- [35] Barthlott, W., Neinhuis, C., *Planta*, 202: (1997) 1
- [36] Bico, J., Marzolin, C., Quere, D., *Europhys. Lett.*, 47: (1999) 220
- [37] Herminghaus, S., *Europhys. Lett.*, 52: 165 (2000)